

COMSCOPE

BROOKHAVEN
NATIONAL LABORATORY



U.S. DEPARTMENT OF
ENERGY

Global phase diagram of a spin-orbital Kondo impurity model and the suppression of Fermi-liquid scale

Yilin Wang

Brookhaven National Laboratory (BNL)

11/04/2019

Y. Wang *et al.* arXiv: 1910.13643

Elias Walter *et al.* arXiv:1908.04362

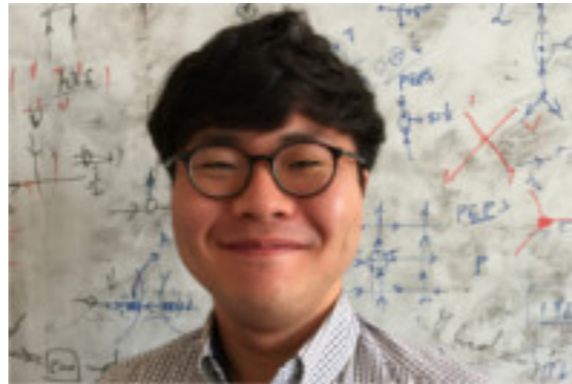
Center for Computational Material Spectroscopy and Design

Collaborators



Elias Walter

Ludwig-Maximilians-Universität
(LMU), Munich



Seung-sup Lee

(LMU)



Katharina Stadler

(LMU)



Jan von Delft

(LMU)



Andreas Weichselbaum

(BNL, LMU)



Gabriel Kotliar

(Rutgers, BNL)

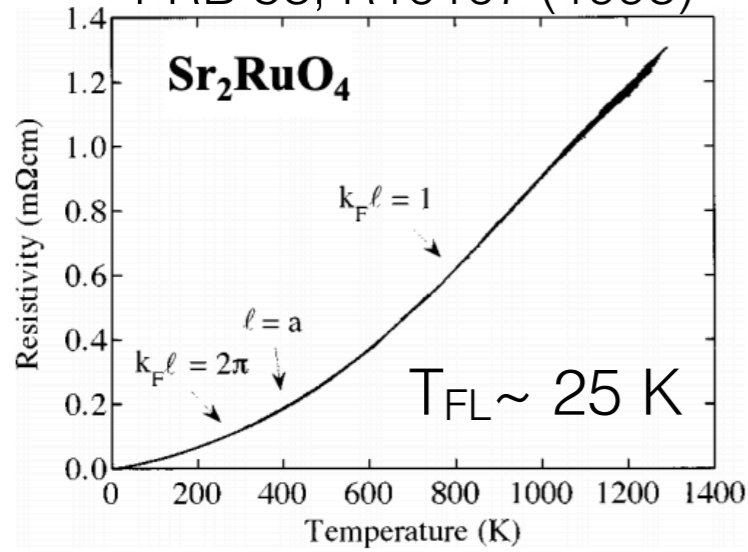
Motivation: very small T_{FL} in many correlated metallic materials

- Many correlated metallic materials can be described by the Landau Fermi-liquid theory at low energies
- but, the Landau Fermi-liquid coherence scale T_{FL} is found to be surprisingly small in many materials
- The Hund metals, including ruthenates, iron-based superconductors, are such class of materials
- For Landau FL theory, below T_{FL} , we would expect that the resistivity will show T^2 law and $\gamma(T)=C(T)/T \sim \text{constant}$

Small coherence scale in Hund metals

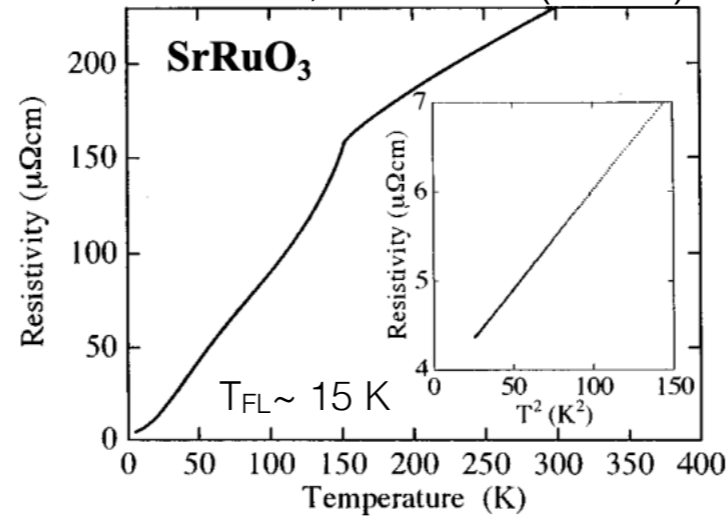
A.W. Tyler et al.

PRB 58, R10107 (1998)



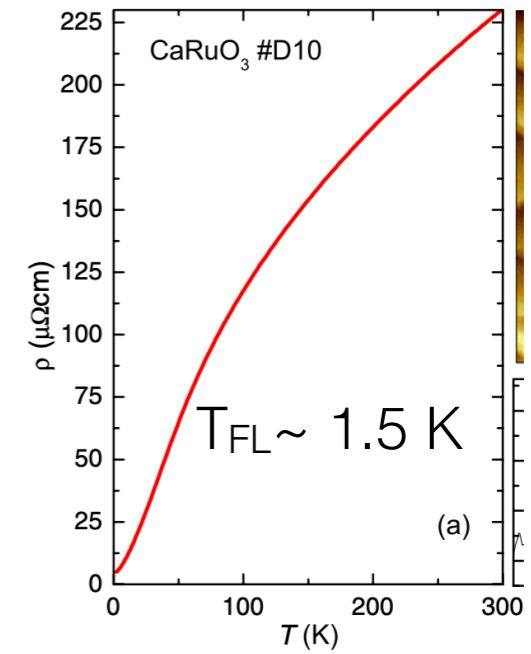
A.P. Mackenzie et al.

PRB 58, R13318 (1998)



M. Schneider et al.

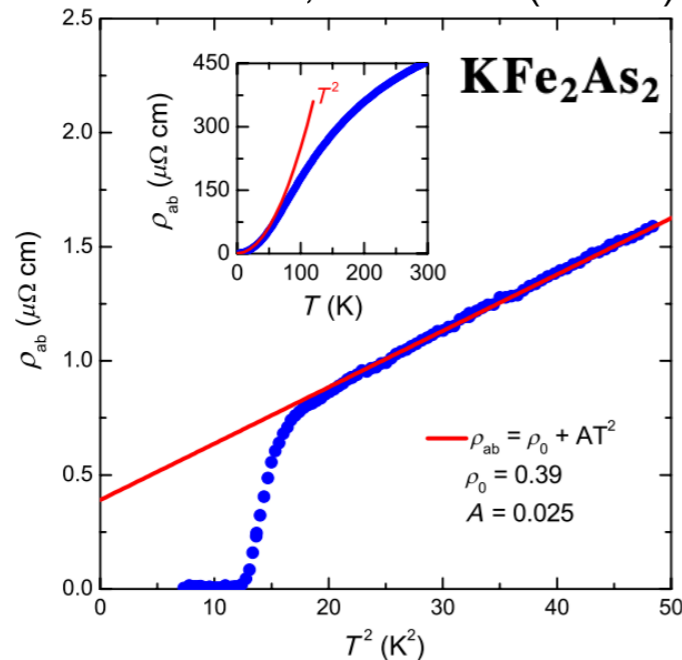
PRL 112, 206403 (2014)



Compound	Magnetic order	$\gamma/\gamma_{\text{LDA}}$	$\rho \propto T^2$	Remarks
Sr_2RuO_4	PM	4	<25 K	Unconventional SC < 1.5 K
SrRuO_3	FM < 160 K	4	<15 K	$\sigma \propto \omega^{-0.5}$
$\text{Sr}_3\text{Ru}_2\text{O}_7$	PM	10	<10 K	Metamagnetic quantum-critical point and nematicity
CaRuO_3	PM	7	$T^{1.5} > 2$ K	$\sigma \propto \omega^{-0.5}, \gamma = \gamma_{\text{FL}} + \log(T)$
Ca_2RuO_4	AF < 110 K	x	x	Insulator < 310 K

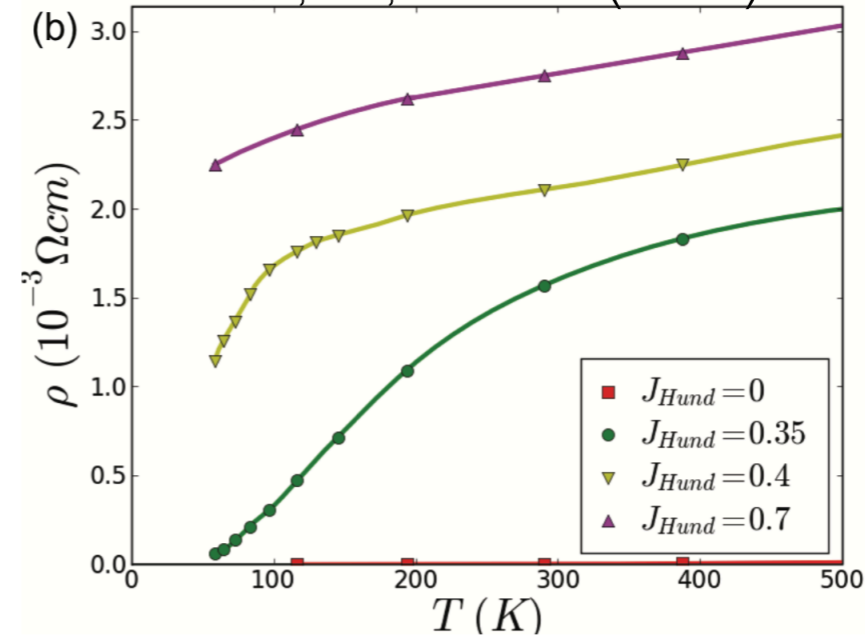
F. Hardy et al.

PRL 111, 027002 (2013)

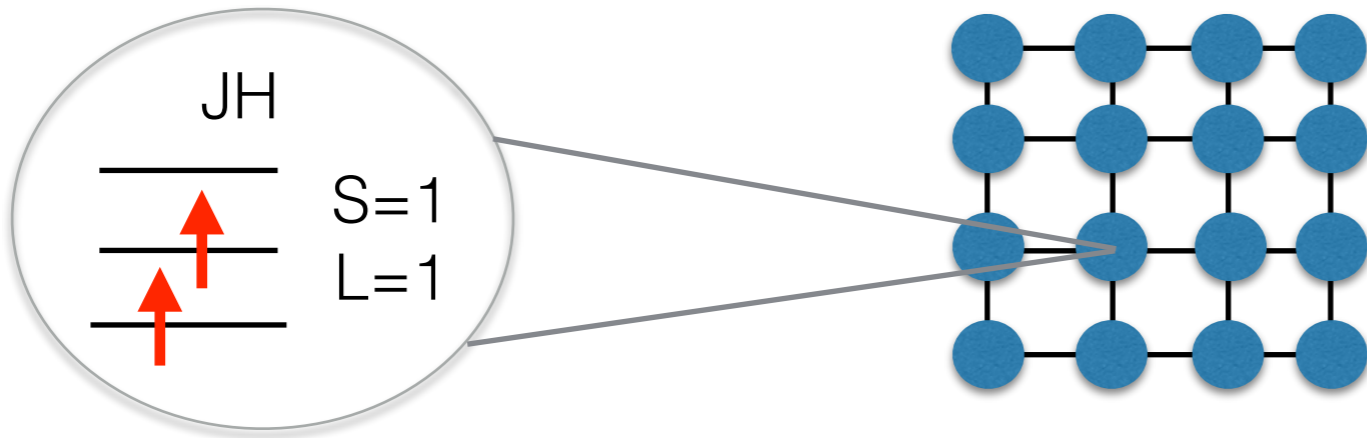


K. Haule and G. Kotliar,

NJP, 11, 025021 (2009)



Hund metals: Strong correlation from Hund's coupling



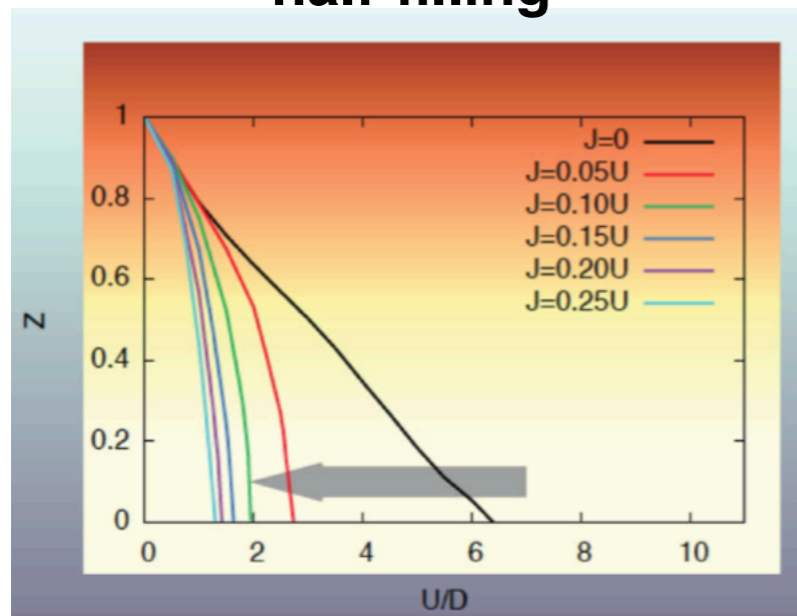
A. Georges *et al.*
Annu. Rev. Condens. Matter Phys.
4, 137–78 (2013)

3-orbital Hubbard Model, DMFT

Luca de' Medici *et al.*, PRL 107, 256401 (2011)

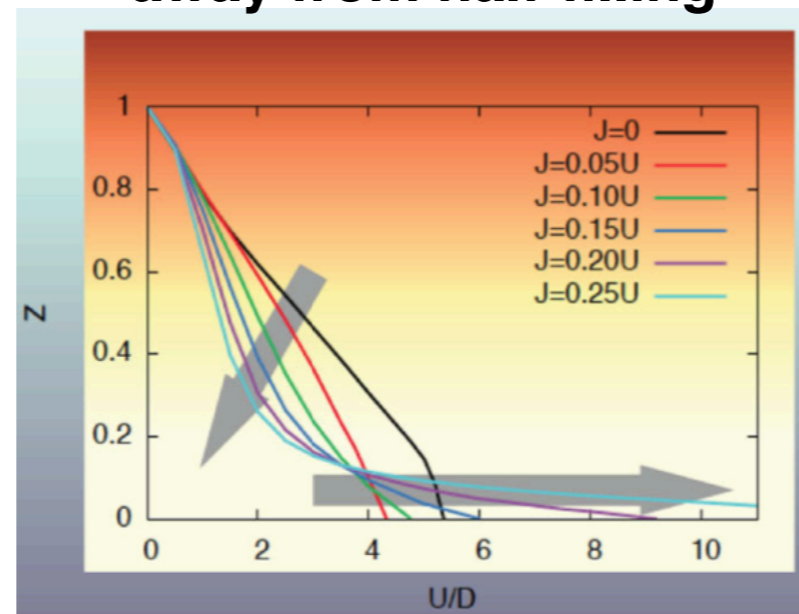
Youichi Yanase *et al.*
JPSJ 66, 3551 (1997)

half-filling

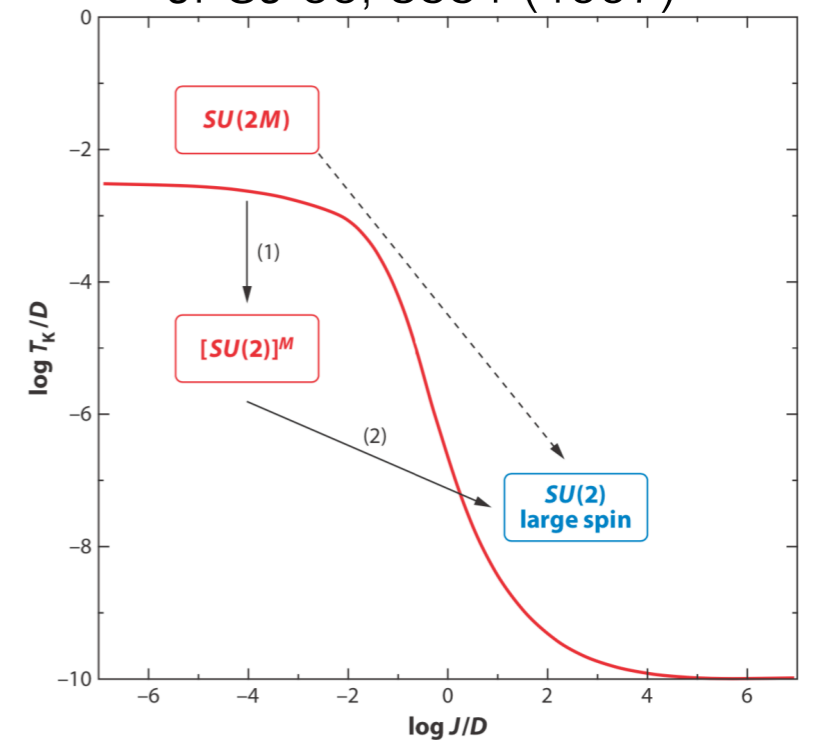


(c) $N = 3$

away from half-filling



(b) $N = 2$



Janus-faced influence of Hund couplings:

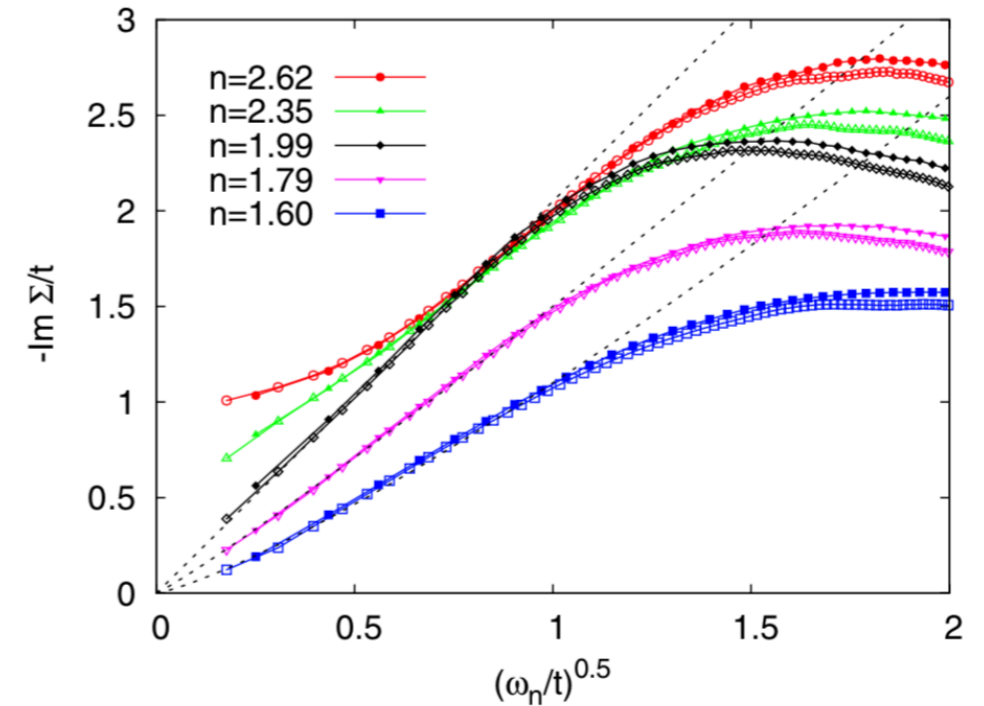
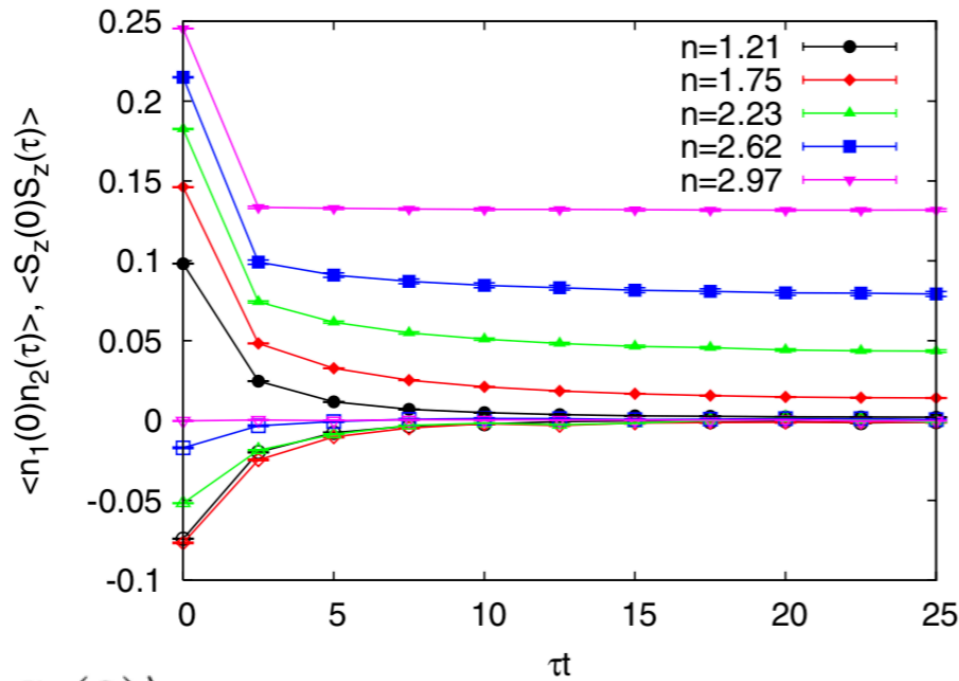
- (1) High energy: It drives the system away from Mott transition
- (2) Low energy: It largely suppresses the coherence scale T_{FL} , above T_{FL} , it shows NFL behavior

$$J_K \propto 1/S$$

$$T_K \propto \exp(-1/J_K)$$

NFL: Spin-freezing and power-law behavior of self-energy above T_{FL}

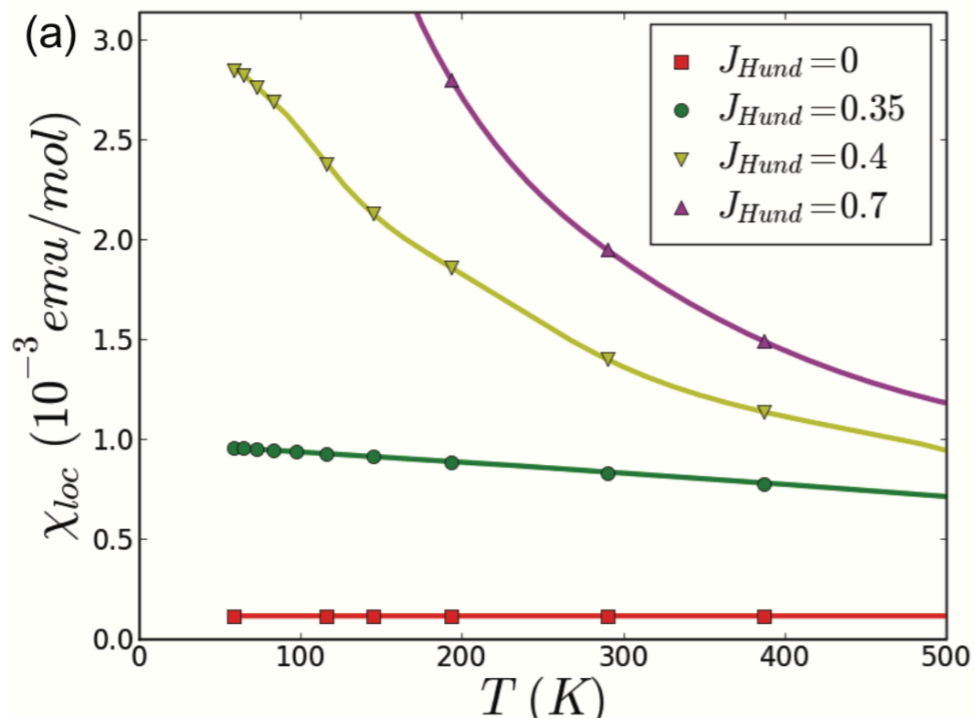
Philipp Werner *et al.* PRL 101, 166405 (2008)



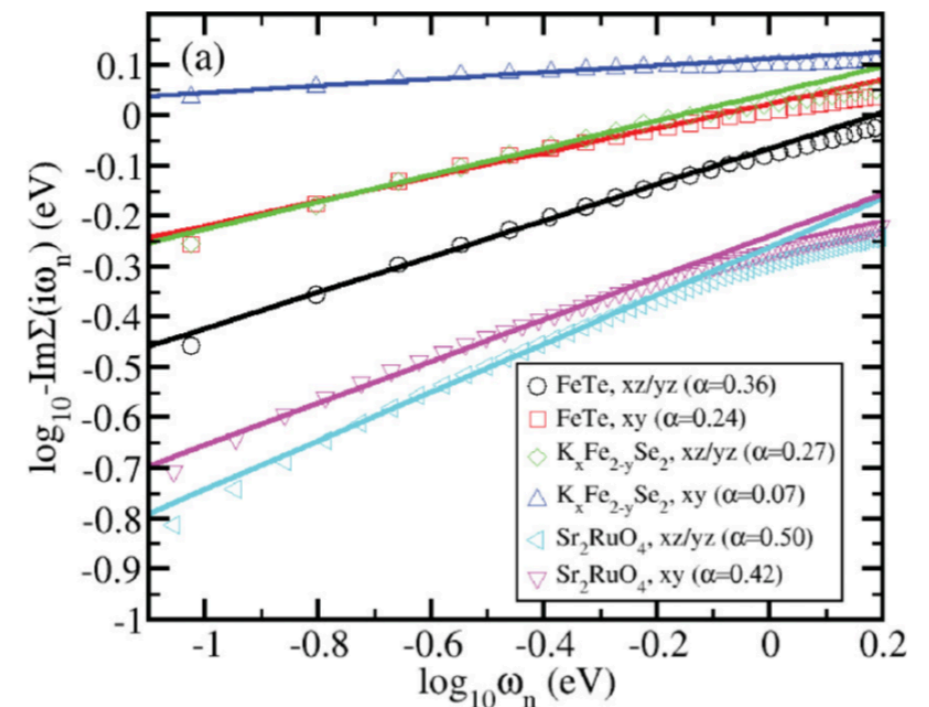
fractional power-law NFL self-energy

$\langle S_z(\tau)S_z(0) \rangle$ saturates to finite value at longer time, indicating frozen moments, “frozen-metal”

K. Haule and G. Kotliar, NJP, 11, 025021 (2009)



Z. P. Yin *et al.* PRB 86, et al.195141 (2012)



Spin-Orbital-Separation (SOS) in Hund metals revealed by DMFT+NRG study

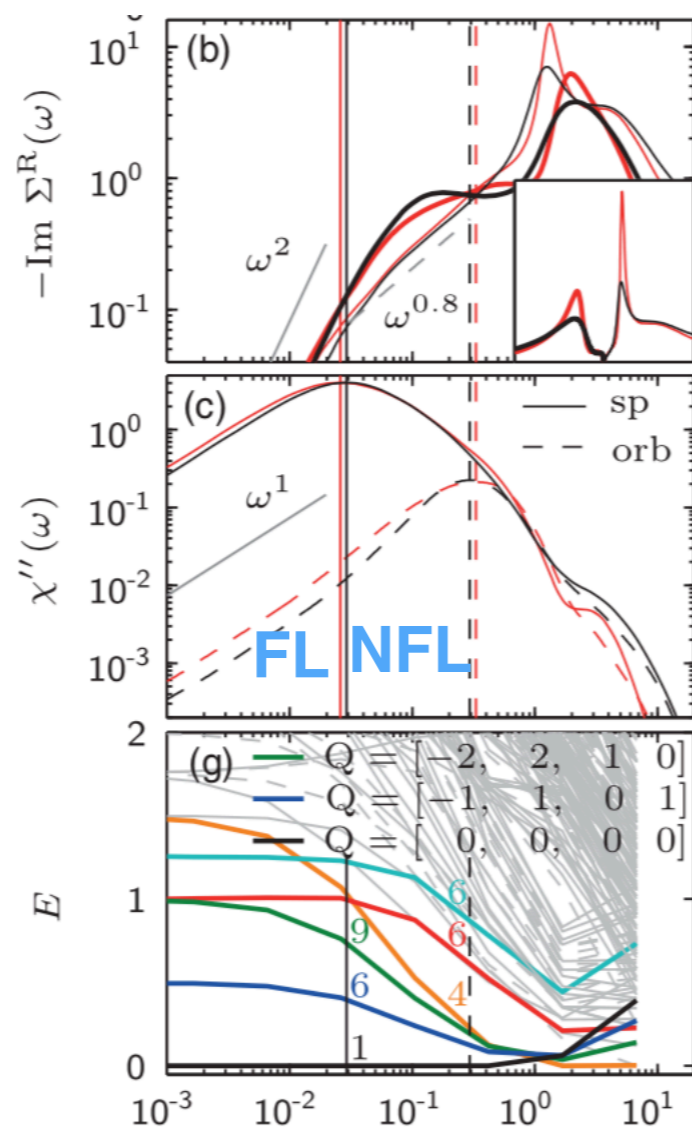
3-orbital Hubbard model K. M. Stadler *et al.* PRL 115, 136401 (2015), Annals of Physics 405, 365 (2019)

$$\hat{H} = \sum_i (-\mu \hat{N}_i + \hat{H}_{\text{int}}[\hat{d}_{i\nu}^\dagger]) + \sum_{\langle ij \rangle \nu} t \hat{d}_{i\nu}^\dagger \hat{d}_{j\nu}, \quad (1a)$$

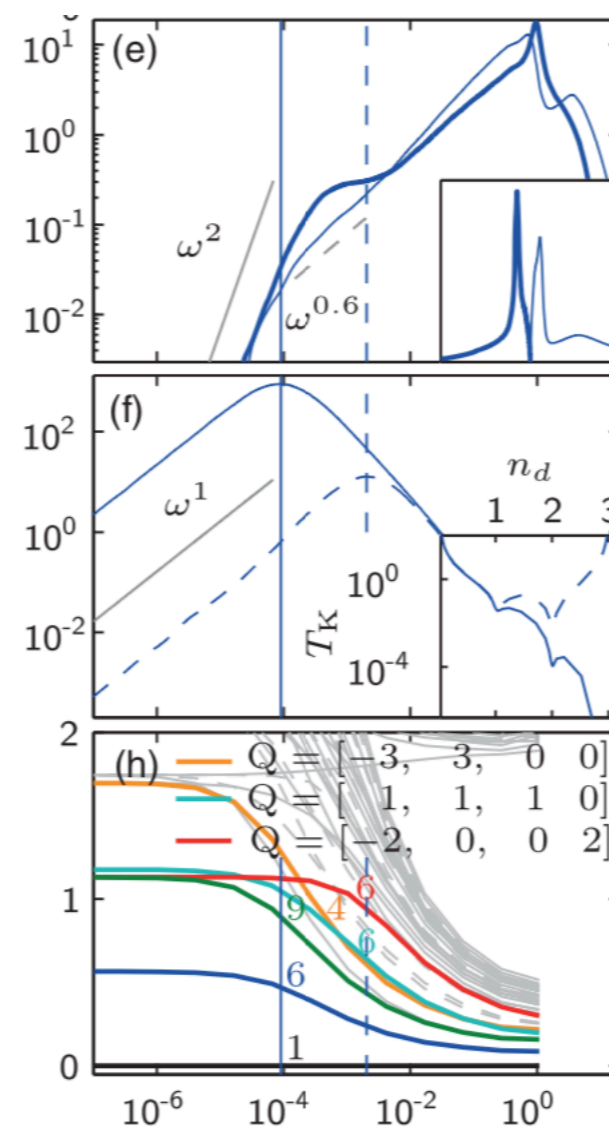
$U(1)_{\text{ch}} \times SU(2)_{\text{sp}} \times SU(3)_{\text{orb}}$ symmetry

$$\hat{H}_{\text{int}}[\hat{d}_{i\nu}^\dagger] = \frac{3}{4} J \hat{N}_i + \frac{1}{2} \left(U - \frac{1}{2} J \right) \hat{N}_i (\hat{N}_i - 1) - J \hat{S}_i^2. \quad (1b)$$

left: with DMFT
self-consistency



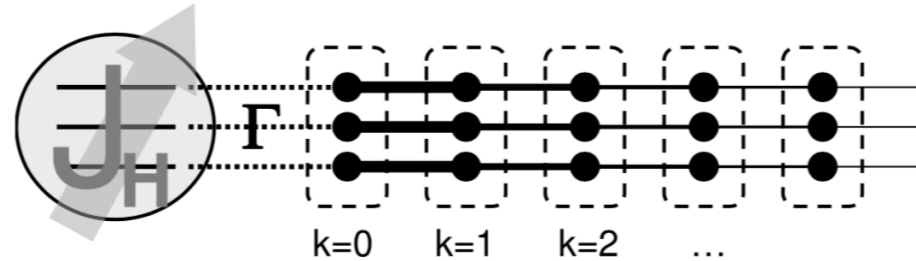
right: without DMFT
self-consistency,
one-shot solution of
Anderson model



Open questions

- The solution of the (LDA+) DMFT equations is a complex problem, which generically yields a non-zero FL scale
- How to reduce the FL scale to exactly zero ?
- How to characterize the ensuing anomalous NFL behavior above T_{FL} ?

NRG computational details



- The bath is discretized logarithmically and mapped to a semi-infinite “Wilson chain” with exponentially decaying hoppings, and the impurity coupled to chain site $k=0$.
- The chain is diagonalized iteratively (adding one more site each iteration), while discarding high-energy states, thereby zooming in on low-energy properties: the finite-size level spacing of a chain ending at site $k \geq 0$ is of order $\omega_k \propto \Lambda^{-k/2}$
- Here $\Lambda > 1$ is a discretization parameter chosen to be 4 in this work.
- The RG flow can be visualized by plotting the rescaled low-lying NRG eigenlevel spectra, $E = (\mathcal{E} - \mathcal{E}_{\text{ref}})/\omega_k$ vs. ω_k , as increasing even or odd k

The imaginary part of dynamical susceptibilities at the impurity site or zeroth bath site at $T=10^{-16}$

$$\chi_{\text{sp}}^{\text{imp,bath}}(\omega) = -\frac{1}{3\pi} \text{Im} \sum_{\alpha} \langle S^{\alpha} || S^{\alpha} \rangle_{\omega},$$

$$\chi_{\text{orb}}^{\text{imp,bath}}(\omega) = -\frac{1}{8\pi} \text{Im} \sum_a \langle T^a || T^a \rangle_{\omega},$$

$$\chi_{\text{sp-orb}}^{\text{imp,bath}}(\omega) = -\frac{1}{24\pi} \text{Im} \sum_{\alpha,a} \langle S^{\alpha} T^a || S^{\alpha} T^a \rangle_{\omega},$$

QSpace tensor library

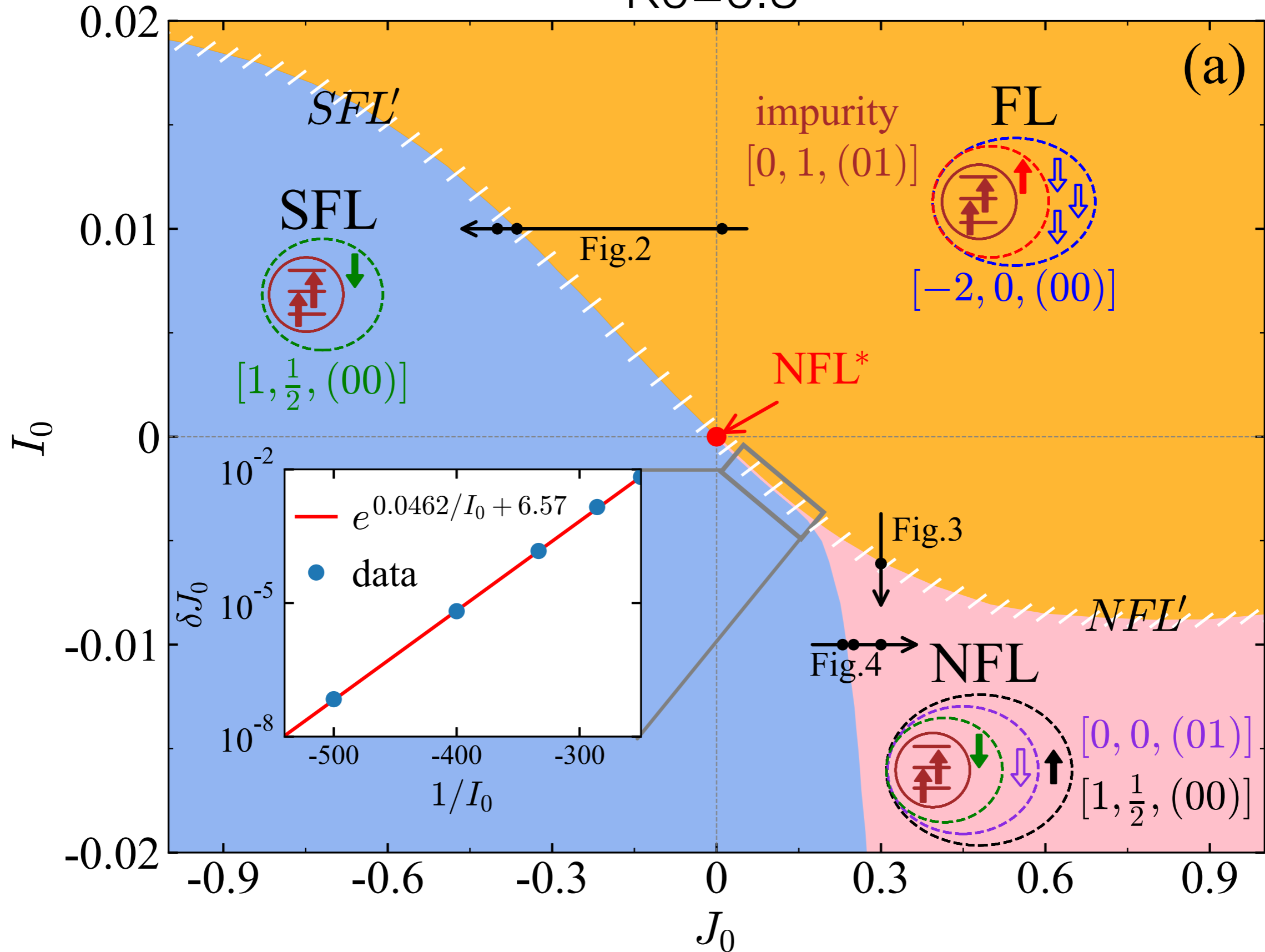
Non-abelian symmetries in tensor networks: A quantum symmetry space approach

Andreas Weichselbaum

[Annals of Physics 327 \(2012\) 2972–3047](#)

Global phase diagram vs. J_0 and I_0

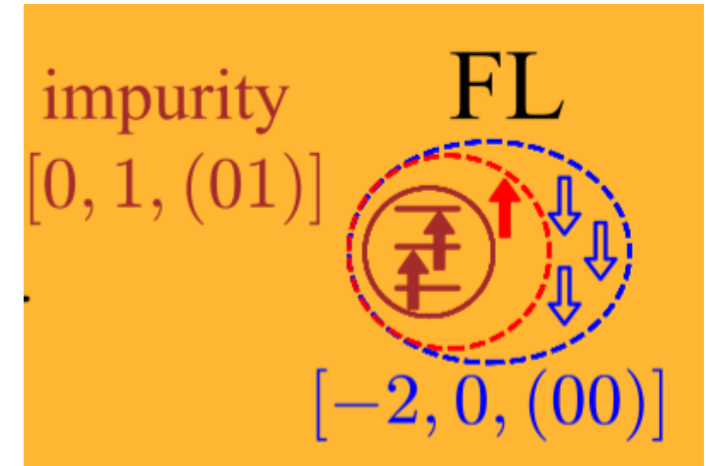
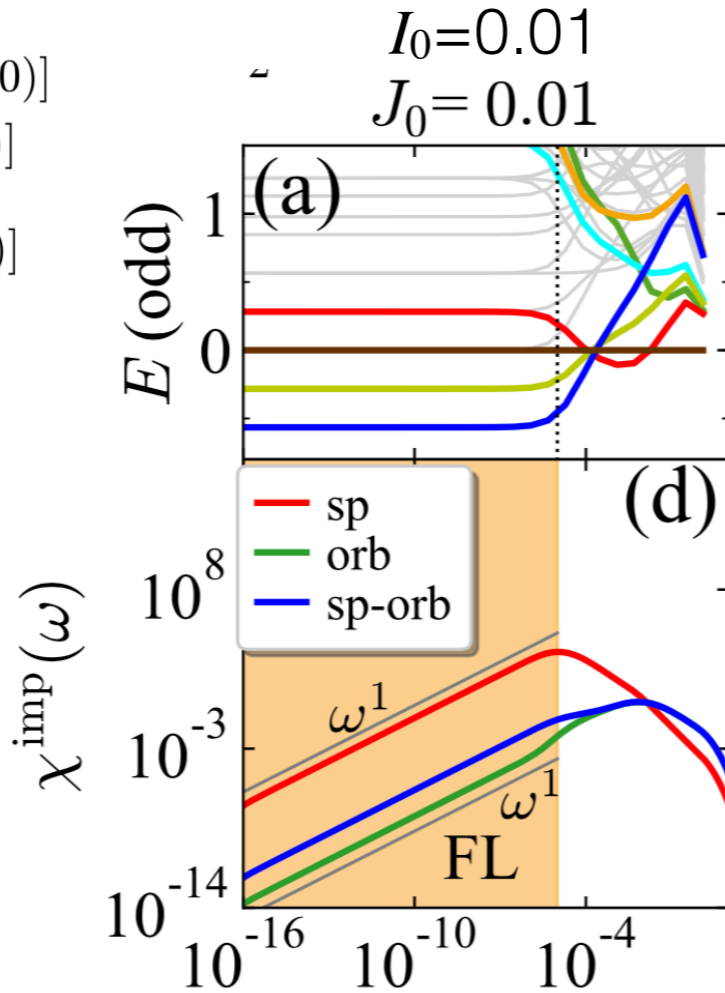
$K_0=0.3$



FL Phase

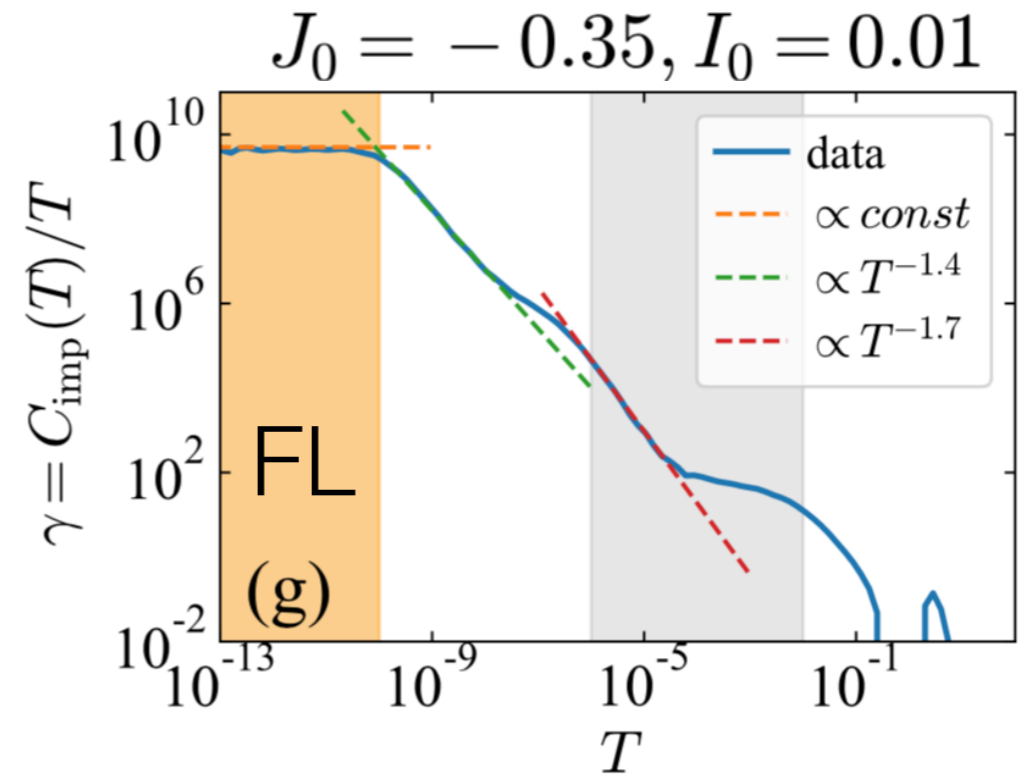
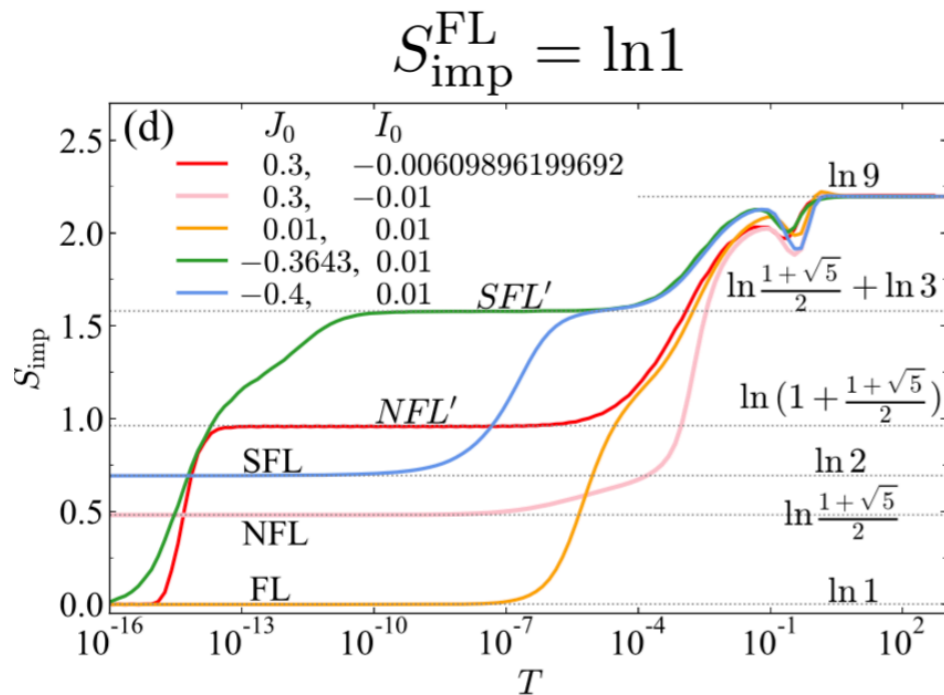
- $[+1, \frac{1}{2}, (00)]$ — $[-1, \frac{3}{2}, (10)]$
- $[+1, \frac{3}{2}, (00)]$ — $[0, 0, (01)]$
- $[-1, \frac{1}{2}, (10)]$ — $[0, 1, (01)]$
- $[-2, 0, (00)]$

gs: $[-2, 0, (00)]$



$$[0, 1, (01)] \otimes [+1, \frac{1}{2}, (10)] \rightarrow [+1, \frac{3}{2}, (00)] \oplus [+1, \frac{1}{2}, (00)]$$

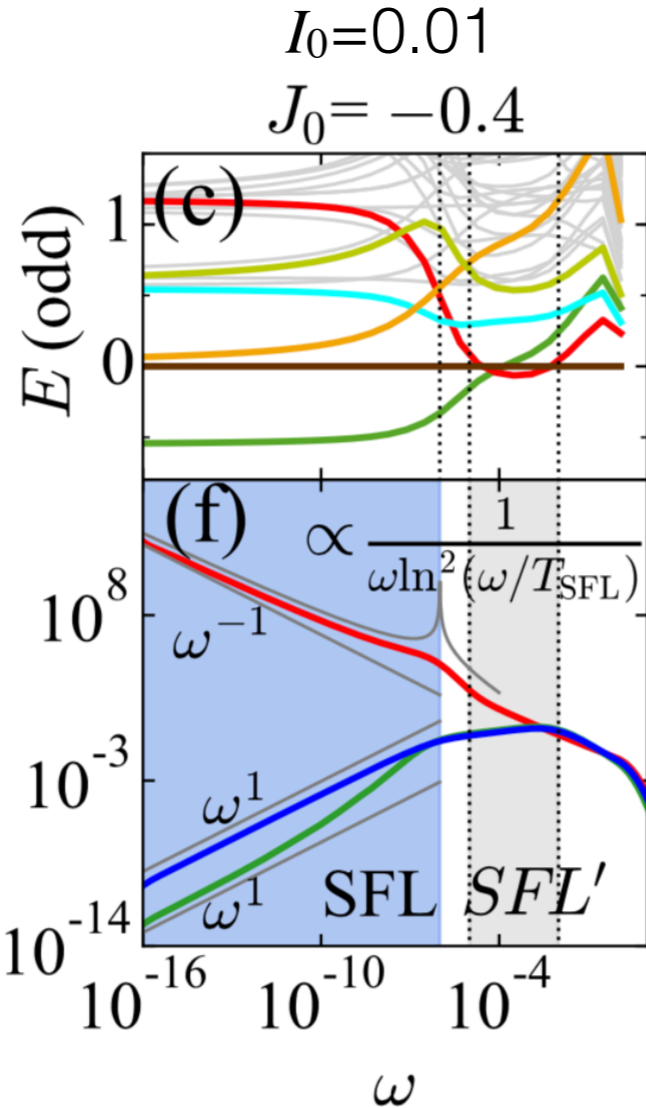
$$[+1, \frac{3}{2}, (00)] \otimes [-3, \frac{3}{2}, (00)] \rightarrow [-2, 0, (00)]$$



Singular-Fermi-liquid (SFL) Phase

- $[+1, \frac{1}{2}, (00)]$ — $[-1, \frac{3}{2}, (10)]$
- $[+1, \frac{3}{2}, (00)]$ — $[0, 0, (01)]$
- $[-1, \frac{1}{2}, (10)]$ — $[0, 1, (01)]$
- $[-2, 0, (00)]$

gs: $[+1, 1/2, (00)]$



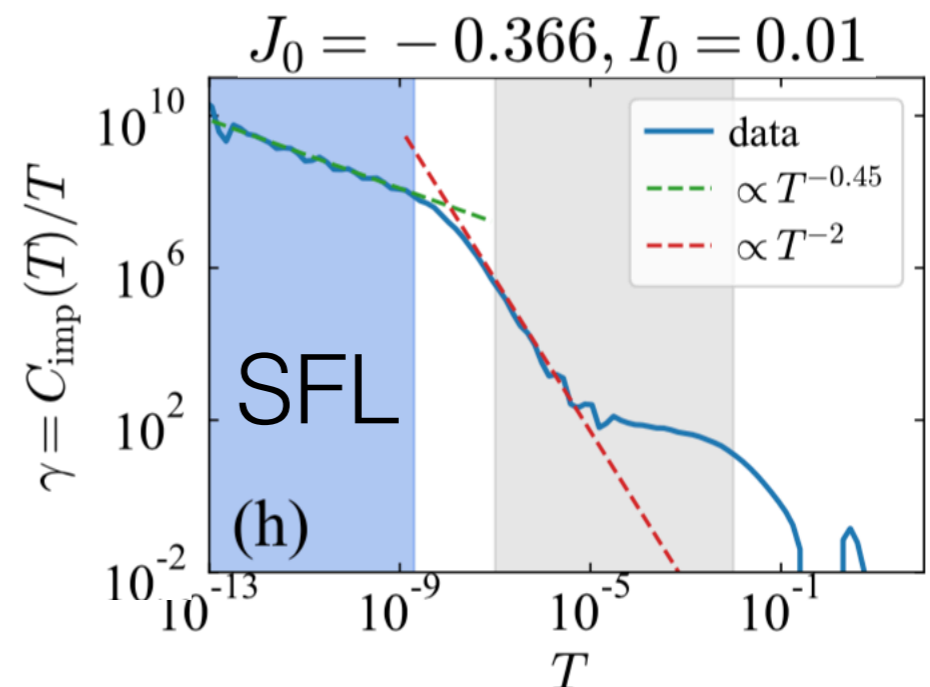
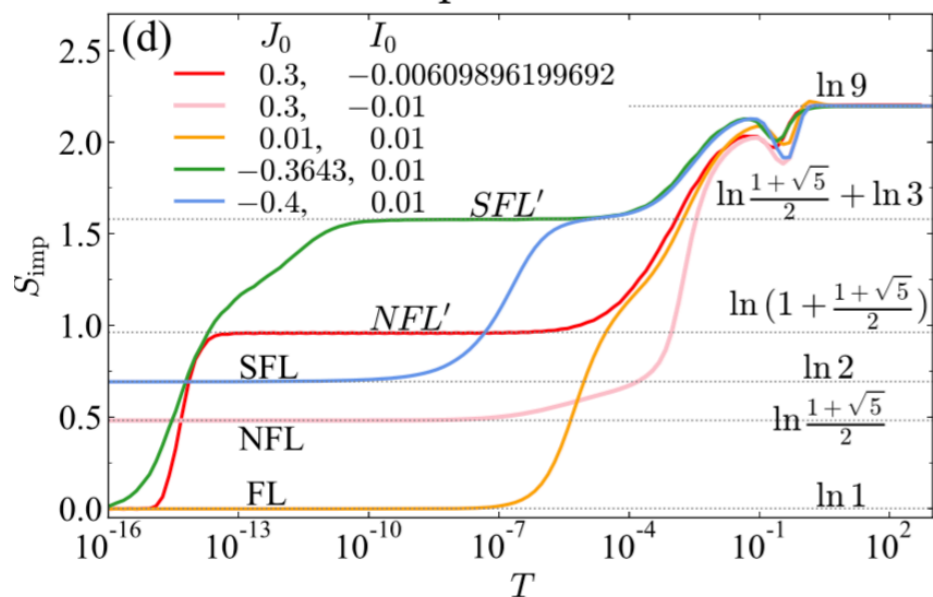
underscreened spin
fully screened orbitals

$$[0, 1, (01)] \otimes [+1, \frac{1}{2}, (10)] \rightarrow [+1, \frac{3}{2}, (00)] \oplus [+1, \frac{1}{2}, (00)]$$

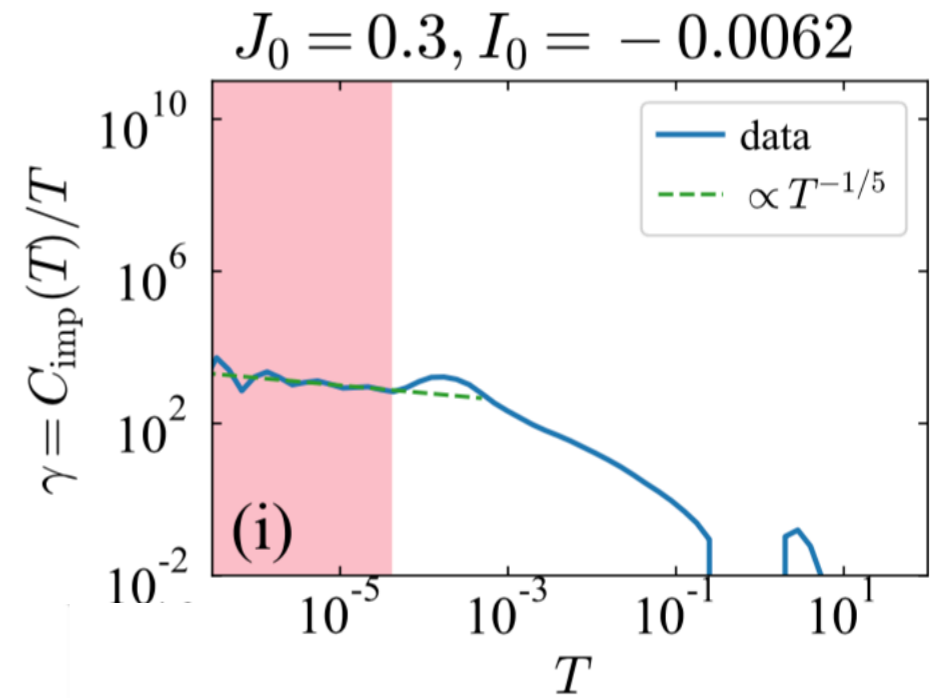
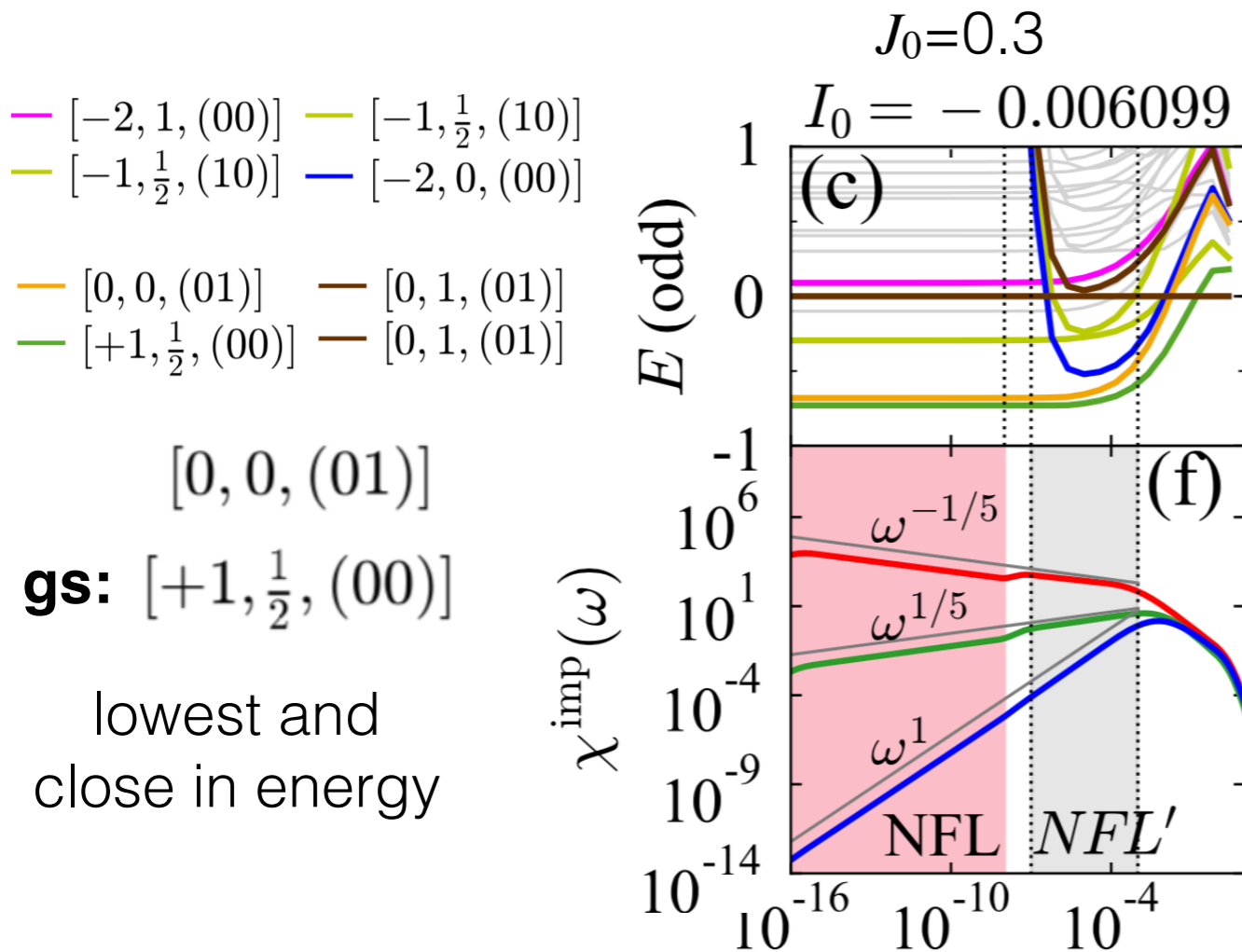
Tensor product of FL spectrum and impurity
 $S=1/2$, with residual effective FM
Kondo couplings in spin sector at
intermediate energies,
showing singular behavior

$$\chi_{\text{sp}}^{\text{imp}} \sim 1/(\omega \ln^2(\omega/T_{\text{SFL}}))$$

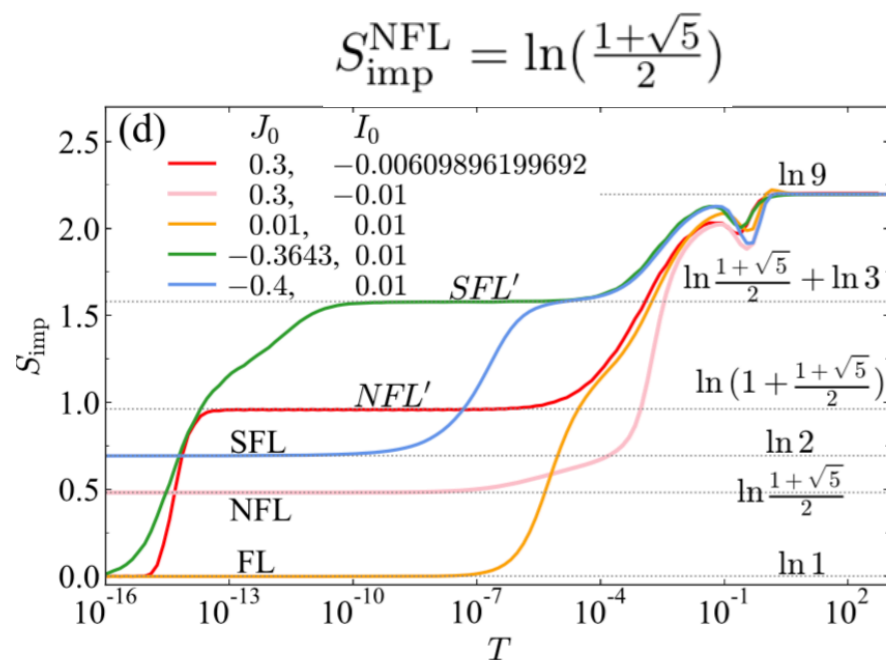
$$S_{\text{imp}}^{\text{SFL}} = \ln 2$$



NFL Phase



Olivier Parcollet *et al.*
 PRB 58,3794 (1998)



general overscreened $SU(N)_K$ Kondo model

$$S_{\text{imp}} = \ln \prod_{n=1}^Q \frac{\sin[\pi(N+1-n)/(N+K)]}{\sin[\pi n/(N+K)]}$$

- $N=3, K=2, Q=2$, $SU(3)_2$ orbital-(01) Kondo model with overscreened fixed point
- $N=2, K=3, Q=1$, $SU(2)_3$ spin-1/2 Kondo model with overscreened fixed point

NFL Phase: Conformal Field Theory (CFT) arguments

Elias *et al.* arXiv:1908.04362

Ian Affleck, Nuclear Physics B 336, 517 (1990)
 Ian Affleck and Andreas Ludwig, Nuclear Physics B 352, 849 (1991)
 Ian Affleck and Andreas Ludwig, Nuclear Physics B 360, 641 (1991)
 D.L. Cox and A. Zawadowski, Advances in Physics 47, 599 (1998)

$$H_{\text{bath}} = a_1 \mathcal{J}_{\text{ch}}^\dagger \mathcal{J}_{\text{ch}} + a_2 \mathcal{J}_{\text{sp}}^\dagger \mathcal{J}_{\text{sp}} + a_3 \mathcal{J}_{\text{orb}}^\dagger \mathcal{J}_{\text{orb}}$$

$U(1)_{\text{ch}} \times SU(2)_{\text{sp}} \times SU(3)_{\text{orb}}$ symmetry

$$Q \equiv [q, S, (\lambda_1 \lambda_2)]$$

low-energy fixed point Hamiltonian

$$\tilde{\mathcal{J}}_{\text{sp}} = \mathcal{J}_{\text{sp}} + S_{\text{imp}} \quad \tilde{\mathcal{J}}_{\text{orb}} = \mathcal{J}_{\text{orb}} + T_{\text{imp}}$$

$$E(Q; \delta q) = \frac{1}{12}(q + \delta q)^2 + \frac{1}{5}\kappa_2(S) + \frac{1}{5}\kappa_3(\lambda_1, \lambda_2),$$

$$H = H_{\text{bath}} + H_{\text{int}} = a_1 \tilde{\mathcal{J}}_{\text{ch}}^\dagger \tilde{\mathcal{J}}_{\text{ch}} + a_2 \tilde{\mathcal{J}}_{\text{sp}}^\dagger \tilde{\mathcal{J}}_{\text{sp}} + a_3 \tilde{\mathcal{J}}_{\text{orb}}^\dagger \tilde{\mathcal{J}}_{\text{orb}}$$

$$\kappa_2(S) = S(S+1),$$

$$\kappa_3(\lambda_1, \lambda_2) = \frac{1}{3}(\lambda_1^2 + \lambda_2^2 + \lambda_1 \lambda_2 + 3\lambda_1 + 3\lambda_2),$$

Single-Fusion

Double-Fusion

free Fermion
spectrum

effective
impurity
multiplet

NRG
fixed-point
spectrum

dual representation
of effective
impurity
multiplet

CFT boundary
operators
 \hat{O}

$$Q \equiv [q, S, (\lambda_1 \lambda_2)] \otimes Q_{\text{imp}}^{\text{eff}} \rightarrow Q' \equiv [q', S', (\lambda'_1 \lambda'_2)] \otimes \bar{Q}_{\text{imp}}^{\text{eff}} \rightarrow Q'' \equiv [q'', S'', (\lambda''_1 \lambda''_2)]$$

$$E(Q; 0)$$

$$E(Q'; \delta q)$$

$$\Delta = E(Q''; \delta q)$$

Scheme I, $SU(2)_3$ fusion in spin sector with

$$Q_{\text{imp}}^{\text{eff}} = [+1, \frac{1}{2}, (00)] \quad \bar{Q}_{\text{imp}}^{\text{eff}} = [-1, \frac{1}{2}, (00)]$$

Scheme II, $SU(3)_2$ fusion in orbital sector with

$$Q_{\text{imp}}^{\text{eff}} = [0, 0, (01)] \quad \bar{Q}_{\text{imp}}^{\text{eff}} = [0, 0, (10)]$$

CFT results of NFL phase: $SU(2)_3$ fusion in spin sector

$$J_0=0.3, I_0=-0.01$$

free fermions					single fusion, with $Q_{\text{imp}}^{\text{eff}} = [+1, \frac{1}{2}, (00)]$					NRG	double fusion, with $\bar{Q}_{\text{imp}}^{\text{eff}} = [-1, \frac{1}{2}, (00)]$					
q	S	$(\lambda_1\lambda_2)$	d	E	q'	S'	$(\lambda'_1\lambda'_2)$	d'	E'	$\delta E'$	E_{NRG}	q''	S''	$(\lambda''_1\lambda''_2)$	Δ	\hat{O}
0	0	(00)	1	0	+1	$\frac{1}{2}$	(00)	2	$\frac{7+5\delta q}{30}$	0	0	0	0	(00)	0	$\mathbb{1}$
												0	1	(00)	$\frac{2}{5} (= \Delta_{\text{sp}})$	Φ_{sp}
+1	$\frac{1}{2}$	(10)	6	$\frac{1}{2}$	+2	0	(10)	3	$\frac{9+5\delta q}{15}$	$\frac{11+5\delta q}{30}$ (0.374)	0.369	+1	$\frac{1}{2}$	(10)	$\frac{3+\delta q}{6}$	
					+2	1	(10)	9	$\frac{3+\delta q}{3}$	$\frac{23+5\delta q}{30}$ (0.774)	0.809	+1	$\frac{1}{2}$	(10)	$\frac{3+\delta q}{6}$	
-1	$\frac{1}{2}$	(01)	6	$\frac{1}{2}$	0	0	(01)	3	$\frac{4}{15}$	$\frac{1-5\delta q}{30}$ (0.026)	0.026	-1	$\frac{1}{2}$	(01)	$\frac{3-\delta q}{6}$	
					0	1	(01)	9	$\frac{2}{3}$	$\frac{13-5\delta q}{30}$ (0.426)	0.422	-1	$\frac{1}{2}$	(01)	$\frac{3-\delta q}{6}$	
												-1	$\frac{3}{2}$	(01)	$\frac{33-5\delta q}{30}$	
0	1	(11)	24	1	+1	$\frac{1}{2}$	(11)	16	$\frac{5+\delta q}{6}$	$\frac{3}{5}$ (0.600)	0.600	0	0	(11)	$\frac{3}{5} (= \Delta_{\text{orb}})$	Φ_{orb}
					0	1	(11)	11	$\frac{33-5\delta q}{30}$			0	1	(11)	$1 (= \Delta_{\text{sp-orb}})$	$\Phi_{\text{sp-orb}}$
												+1	$\frac{3}{2}$	(11)	$\frac{43+5\delta q}{30}$	$\frac{6}{5}$ (1.200)
+2	0	(20)	6	1	+3	$\frac{1}{2}$	(20)	12	$\frac{47+15\delta q}{30}$	$\frac{4+\delta q}{3}$ (1.348)	1.432	+2	0	(20)	$\frac{3+\delta q}{3}$	
					+2	1	(20)	15	$\frac{21+5\delta q}{15}$			+2	1	(20)	$\frac{21+5\delta q}{15}$	
-2	0	(02)	6	1	-1	$\frac{1}{2}$	(02)	12	$\frac{27-5\delta q}{30}$	$\frac{2-\delta q}{3}$ (0.652)	0.655	-2	0	(02)	$\frac{3-\delta q}{3}$	
					-2	1	(02)	15	$\frac{21-5\delta q}{15}$			-2	1	(02)	$\frac{21-5\delta q}{15}$	
+2	1	(01)	9	1	+3	$\frac{1}{2}$	(01)	6	$\frac{7+3\delta q}{6}$	$\frac{14+5\delta q}{15}$ (0.948)	0.954	+2	0	(01)	$\frac{9+5\delta q}{15}$	
					+3	$\frac{3}{2}$	(01)	12	$\frac{53+15\delta q}{30}$	$\frac{23+5\delta q}{15}$ (1.548)	1.599	+2	1	(01)	$\frac{3+\delta q}{3}$	
-2	1	(10)	9	1	-1	$\frac{1}{2}$	(10)	6	$\frac{3-\delta q}{6}$	$\frac{4-5\delta q}{15}$ (0.252)	0.248	-2	0	(10)	$\frac{9-5\delta q}{15}$	
					-2	1	(10)	10	$\frac{3-\delta q}{3}$			-2	1	(10)	$\frac{3-\delta q}{3}$	
												-1	$\frac{3}{2}$	(10)	$\frac{33-5\delta q}{30}$	$\frac{13-5\delta q}{15}$ (0.852)
												-2	1	(10)	$\frac{3-\delta q}{3}$	

$$E_{\text{NRG}}$$

have been shifted and rescaled such that the ground state is zero and the values of E_{NRG} and $\delta E'$ match for the multiplet $[+1, \frac{1}{2}, (11)]$

δq is then determined by matching E_{NRG} and $\delta E'$ for the multiplet $[0, 0, (01)]$

$$\delta q = 0.0433$$

$$E([0, 0, (01)]) - E([+1, \frac{1}{2}, (00)]) = \frac{1-5\delta q}{30}$$

power-laws from CFT

$$\chi_{\text{sp}}^{\text{imp}} \sim \omega^{2\Delta_{\text{sp}}-1} = \omega^{-1/5},$$

$$\chi_{\text{orb}}^{\text{imp}} \sim \omega^{2\Delta_{\text{orb}}-1} = \omega^{1/5},$$

$$\chi_{\text{sp-orb}}^{\text{imp}} \sim \omega^{2\Delta_{\text{sp-orb}}-1} = \omega^1.$$

specific heat coefficient from CFT

$$\gamma(T) \propto T^{2\Delta_{\text{sp}}-1} = T^{-1/5}$$

Olivier Parcollet *et al.*
PRB 58,3794 (1998)

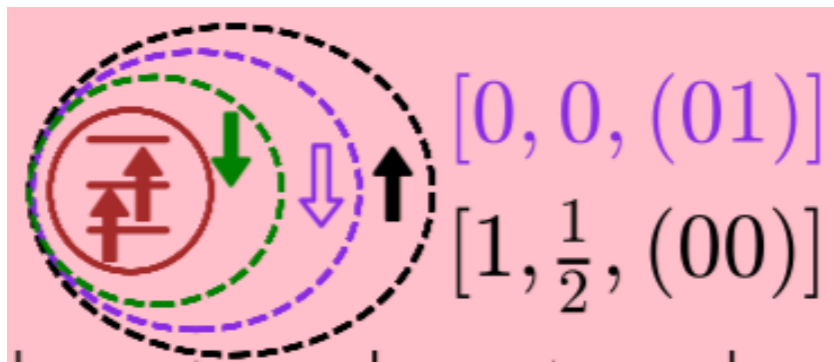
CFT results of NFL phase: $SU(3)_2$ fusion in orbital sector

$$J_0=0.3, I_0=-0.01$$

free fermions					single fusion, with $Q_{\text{imp}}^{\text{eff}} = [0, 0, (01)]$					NRG	double fusion, with $\bar{Q}_{\text{imp}}^{\text{eff}} = [0, 0, (10)]$					
q	S	$(\lambda_1 \lambda_2)$	d	E	q'	S'	$(\lambda'_1 \lambda'_2)$	d'	E'	$\delta E'$	E_{NRG}	q''	S''	$(\lambda''_1 \lambda''_2)$	Δ	\hat{O}
0	0	(00)	1	0	0	0	(01)	3	$\frac{4}{15}$	$\frac{1-5\delta q}{30}$ (0.026)	0.026	0	0	(00)	0	$\mathbb{1}$
												0	0	(11)	$\frac{3}{5}$ ($= \Delta_{\text{orb}}$)	Φ_{orb}
+1	$\frac{1}{2}$	(10)	6	$\frac{1}{2}$	+1	$\frac{1}{2}$	(00)	2	$\frac{7+5\delta q}{30}$	0	0	+1	$\frac{1}{2}$	(10)	$\frac{3+\delta q}{6}$	
					+1	$\frac{1}{2}$	(11)	16	$\frac{5+\delta q}{6}$	$\frac{3}{5}$ (0.600)	0.600	+1	$\frac{1}{2}$	(10)	$\frac{3+\delta q}{6}$	
												+1	$\frac{1}{2}$	(02)	$\frac{27+5\delta q}{30}$	
-1	$\frac{1}{2}$	(01)	6	$\frac{1}{2}$	-1	$\frac{1}{2}$	(10)	6	$\frac{3-\delta q}{6}$	$\frac{4-5\delta q}{15}$ (0.252)	0.248	-1	$\frac{1}{2}$	(01)	$\frac{3-\delta q}{6}$	
					-1	$\frac{1}{2}$	(20)	12	$\frac{27-5\delta q}{30}$	$\frac{2-\delta q}{3}$ (0.652)	0.655	-1	$\frac{1}{2}$	(20)	$\frac{27-5\delta q}{30}$	
												-1	$\frac{1}{2}$	(01)	$\frac{3-\delta q}{6}$	
0	1	(11)	24	1	0	1	(01)	9	$\frac{2}{3}$	$\frac{13-5\delta q}{30}$ (0.426)	0.422	0	1	(00)	$\frac{2}{5}$ ($= \Delta_{\text{sp}}$)	Φ_{sp}
					0	1	(11)	1	$\frac{1}{5}$ ($= \Delta_{\text{sp-orb}}$)	$\Phi_{\text{sp-orb}}$	0	1	(11)	1		
					0	1	(20)	18	$\frac{16}{15}$	$\frac{5-\delta q}{6}$ (0.826)	0.825	0	1	(11)	1	
+2	0	(20)	6	1	+2	0	(10)	3	$\frac{9+5\delta q}{15}$	$\frac{11+5\delta q}{30}$ (0.374)	0.369	+2	0	(01)	$\frac{9+5\delta q}{15}$	
					+2	0	(20)	3	$\frac{3+\delta q}{3}$		+2	0	(20)	$\frac{3+\delta q}{3}$		
-2	0	(02)	6	1	-2	0	(11)	8	$\frac{14-5\delta q}{15}$	$\frac{7-5\delta q}{10}$ (0.678)	0.673	-2	0	(10)	$\frac{9-5\delta q}{15}$	
					-2	0	(02)	3	$\frac{3-\delta q}{3}$		-2	0	(02)	$\frac{3-\delta q}{3}$		
+2	1	(01)	9	1	+2	1	(10)	9	$\frac{3+\delta q}{3}$	$\frac{23+5\delta q}{30}$ (0.774)	0.809	+2	1	(01)	$\frac{3+\delta q}{3}$	
					+2	1	(20)	15	$\frac{21+5\delta q}{15}$		+2	1	(20)	$\frac{21+5\delta q}{15}$		
					+2	1	(02)	18	$\frac{21+5\delta q}{15}$	$\frac{7+\delta q}{6}$ (1.174)	1.180	+2	1	(01)	$\frac{3+\delta q}{3}$	
-2	1	(10)	9	1	-2	1	(00)	3	$\frac{11-5\delta q}{15}$	$\frac{1-\delta q}{2}$ (0.478)	0.470	-2	1	(10)	$\frac{3-\delta q}{3}$	
					-2	1	(10)	10	$\frac{3-\delta q}{3}$		-2	1	(10)	$\frac{3-\delta q}{3}$		
					-2	1	(11)	24	$\frac{4-\delta q}{3}$	$\frac{11-5\delta q}{10}$ (1.078)	1.090	-2	1	(02)	$\frac{21-5\delta q}{15}$	

An effective $SU(2)_3$ spin Kondo model and an effective $SU(3)_2$ orbital Kondo model with overscreened fixed points are equivalent description of this NFL fixed point

Picture of NFL Phase: alternating overscreenings in spin and orbital sector



$$[0, 1, (01)] \otimes [+1, \frac{1}{2}, (10)] \rightarrow [+1, \frac{3}{2}, (00)] \oplus [+1, \frac{1}{2}, (00)]$$

contrast to FL, $[+1, \frac{1}{2}, (00)]$ has lower energy due to strong FM spin-orbital Kondo coupling I_0

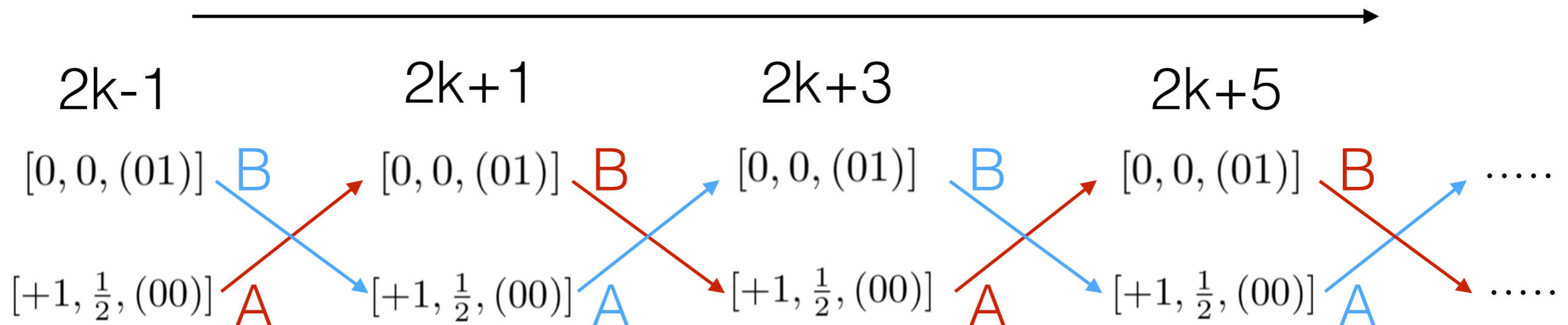
A: bind one hole

$$[+1, \frac{1}{2}, (00)] \otimes [-1, \frac{1}{2}, (01)] \rightarrow [0, 0, (01)]$$

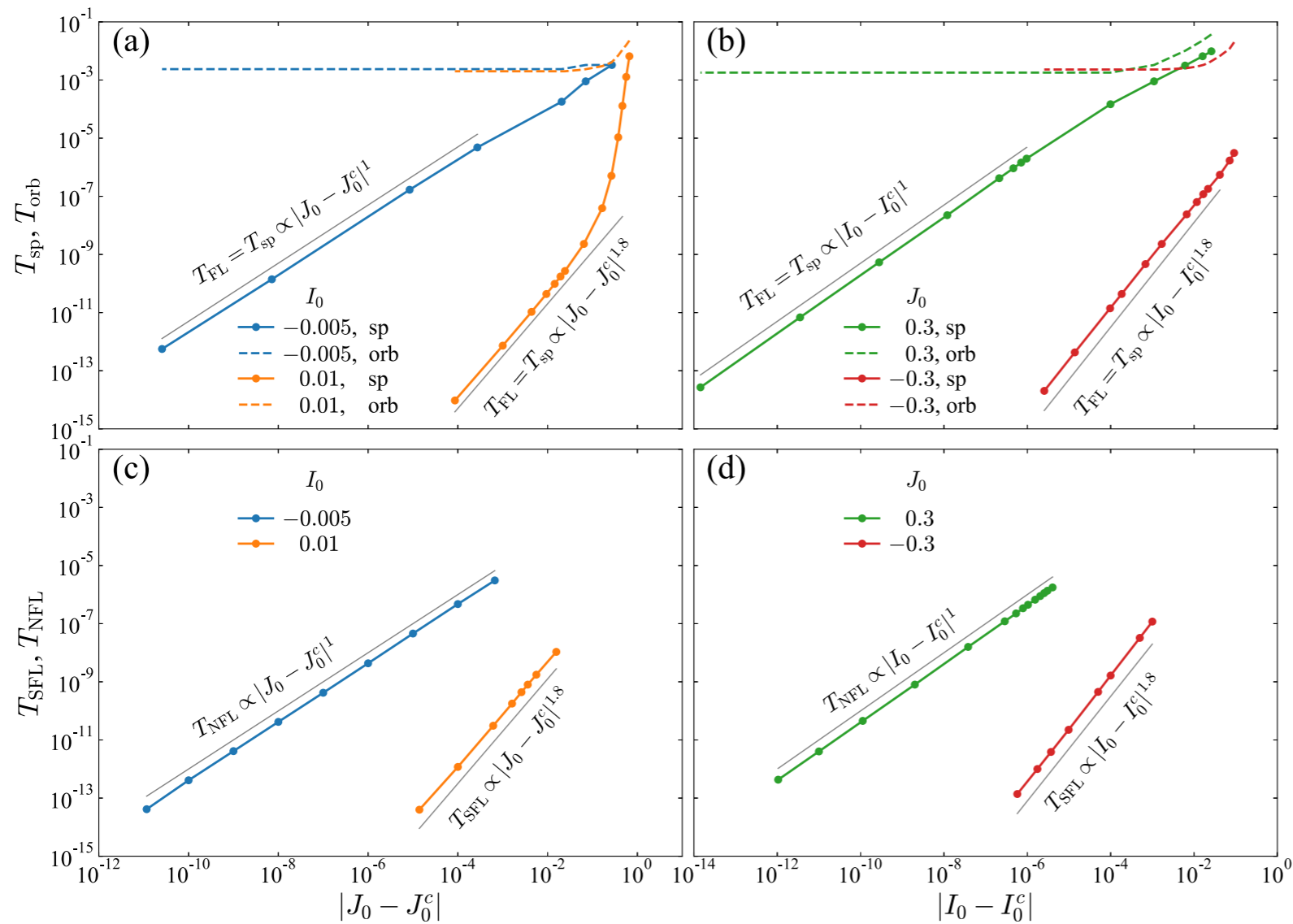
B: bind one electron

$$[0, 0, (01)] \otimes [+1, \frac{1}{2}, (10)] \rightarrow [+1, \frac{1}{2}, (00)]$$

along the Wilson chain with odd-length



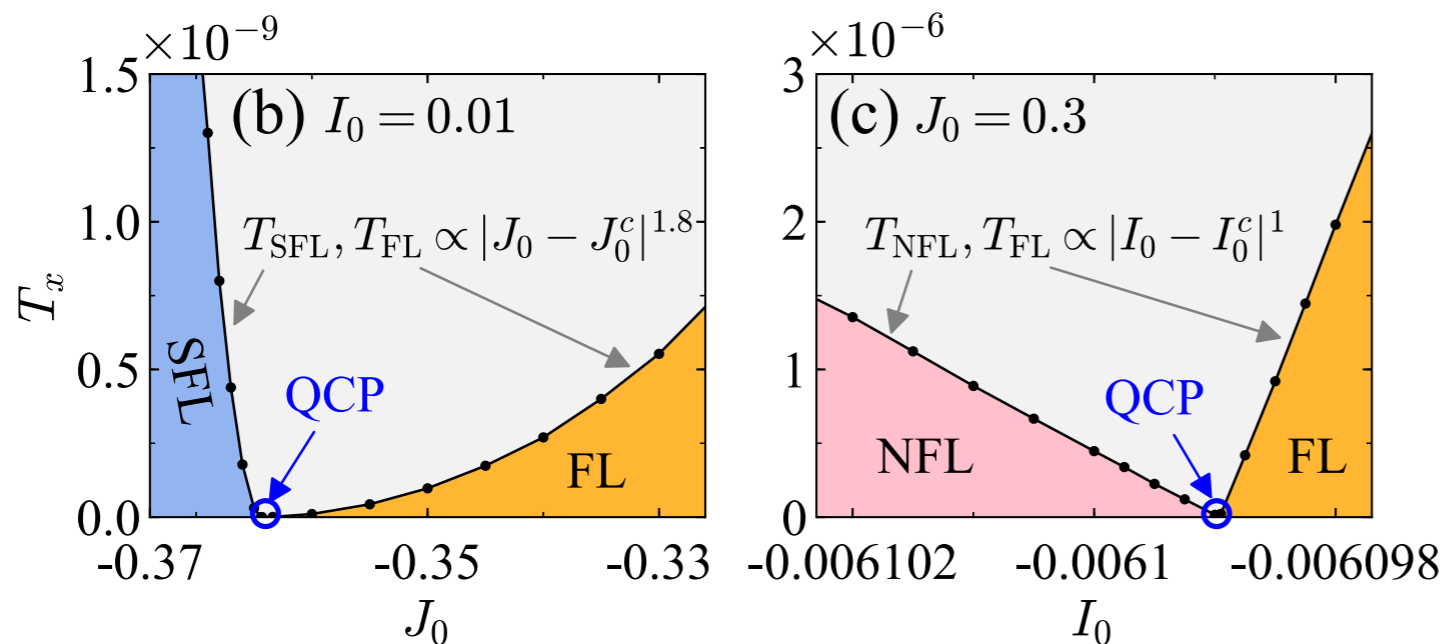
Phase transition: Suppression of FL scale and Quantum Critical Points (QCPs)



$$T_{\text{FL}} = T_{\text{sp}}$$

$$T_{\text{FL/SFL}} \propto |J_0 - J_0^c|^{1.8}, |I_0 - I_0^c|^{1.8},$$

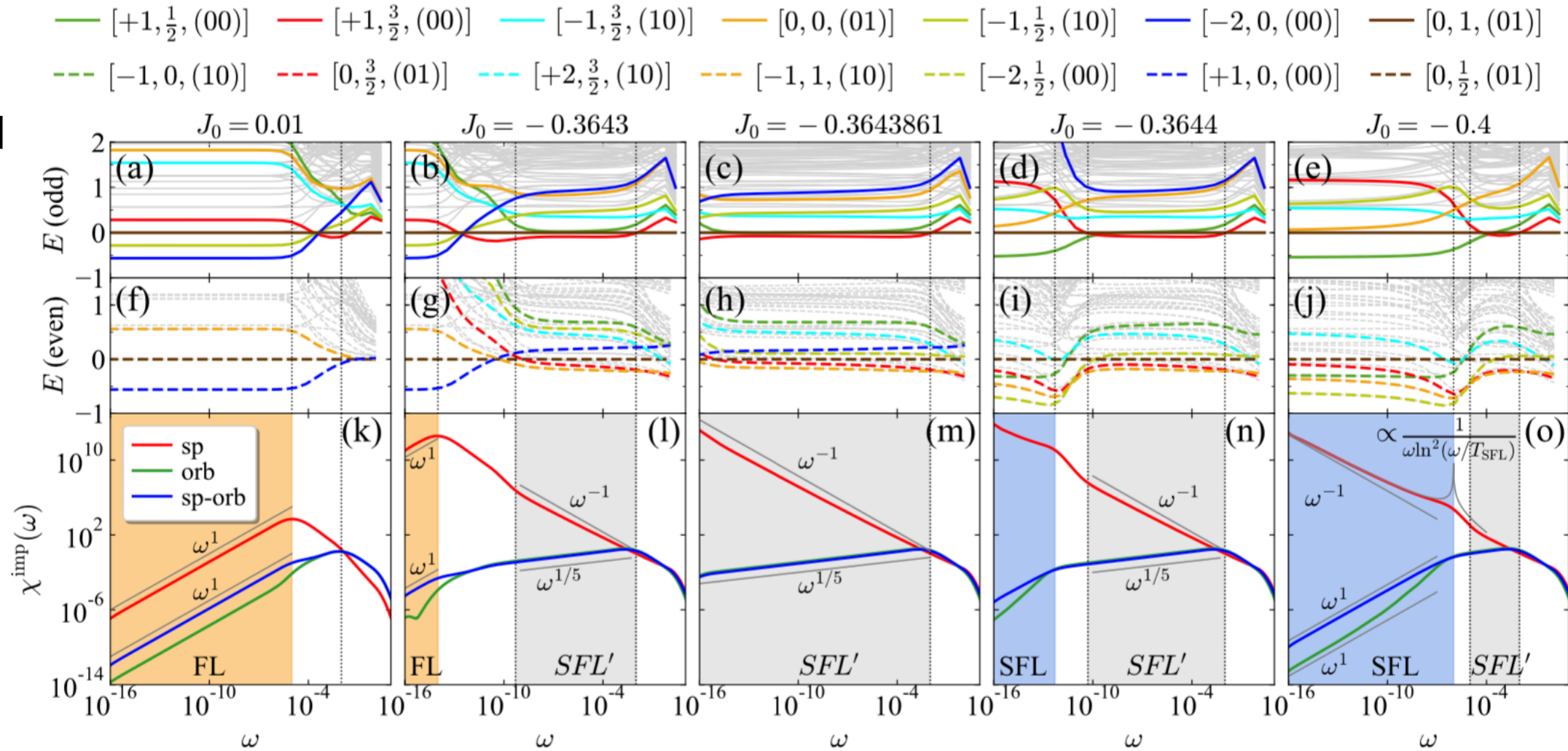
$$T_{\text{FL/NFL}} \propto |J_0 - J_0^c|^1, |I_0 - I_0^c|^1.$$



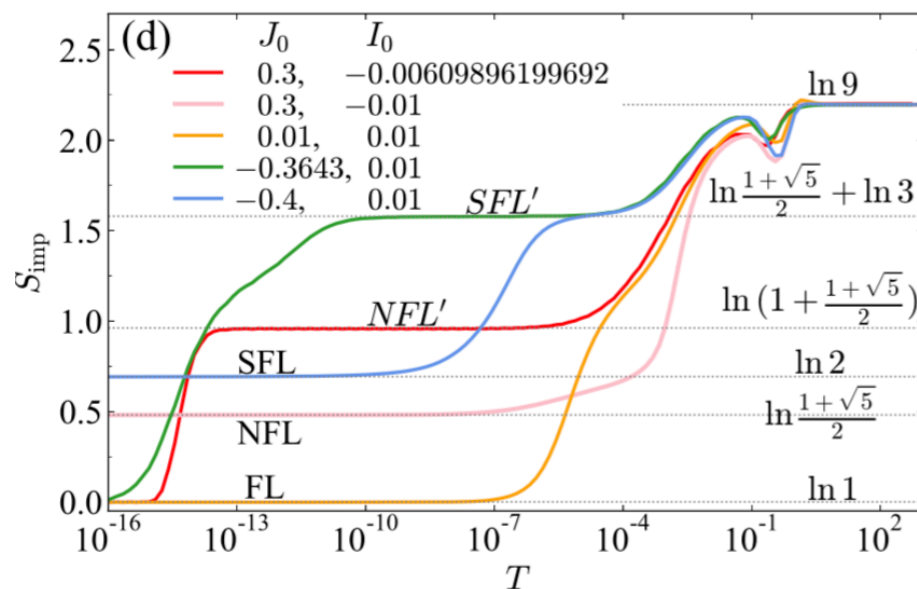
T_{FL} can become arbitrarily small close to these two QCPs

FL to SFL transition, crossover regime SFL' at intermediate energies

$I_0=0.01$



$$S_{\text{imp}}^{SFL'} = \ln \frac{1 + \sqrt{5}}{2} + \ln 3$$



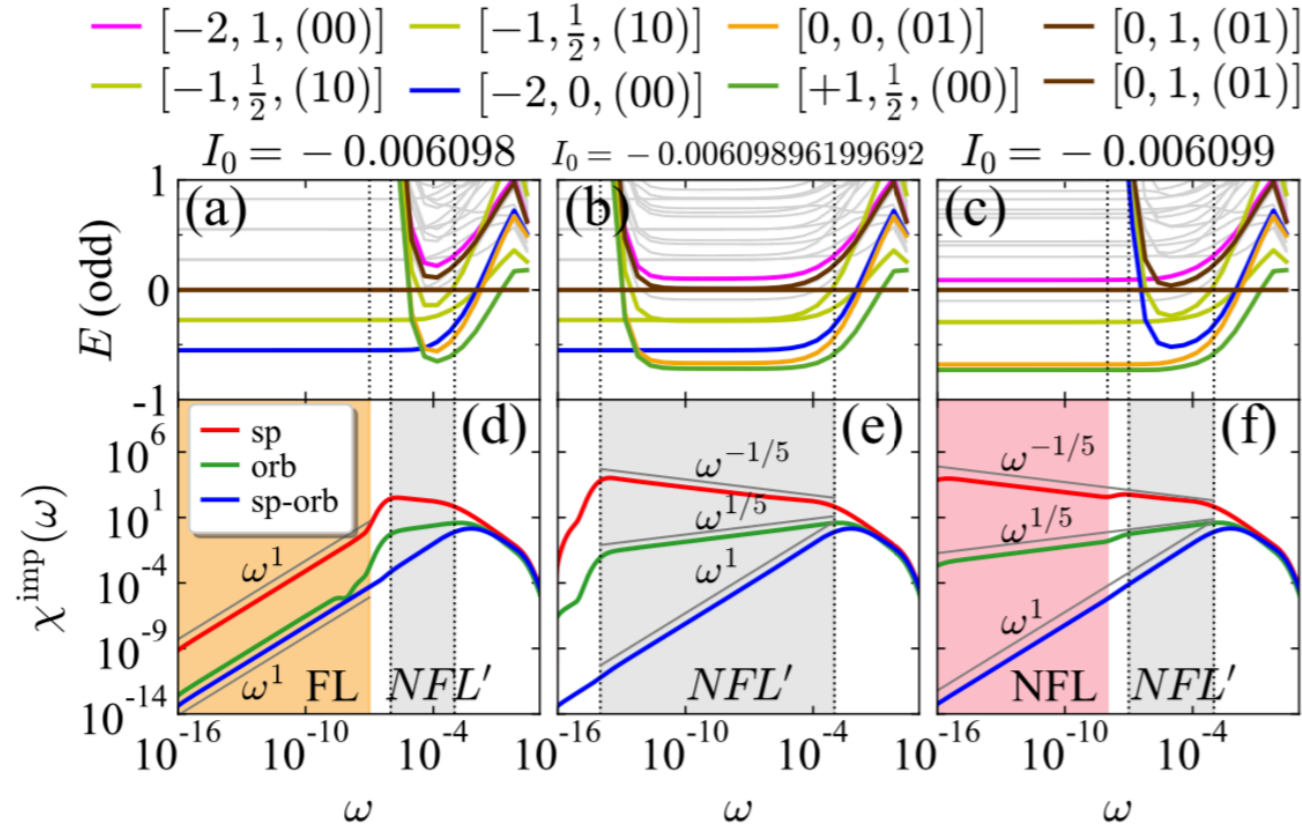
$SU(3)_2$ fixed point with overscreened orbitals and fluctuating spin moment of 1

Alen Horvat et al. arXiv:1907.07100

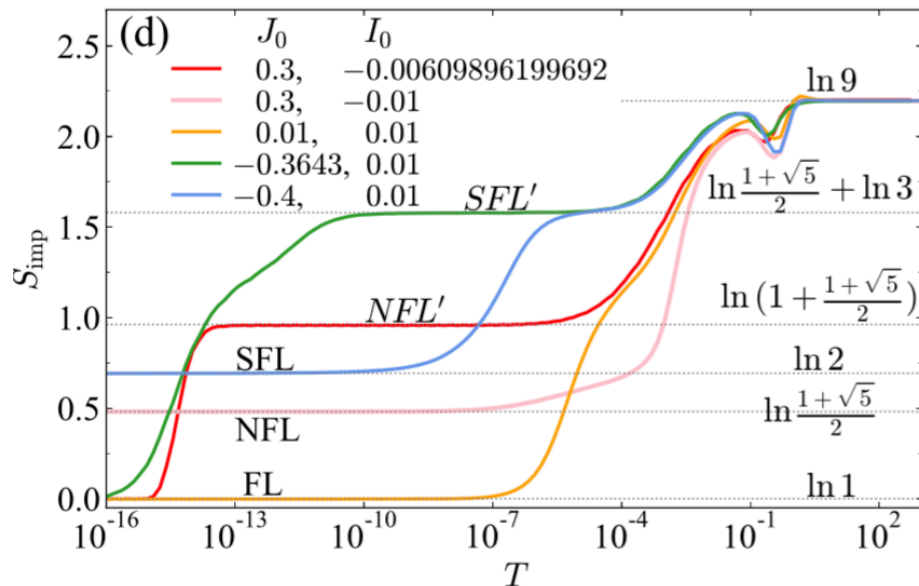
$$I_0 = 0 \quad J_0 \rightarrow 0^+$$

FL to NFL transition, crossover regime NFL' at intermediate energies

$J_0=0.3$



“level-crossing” picture



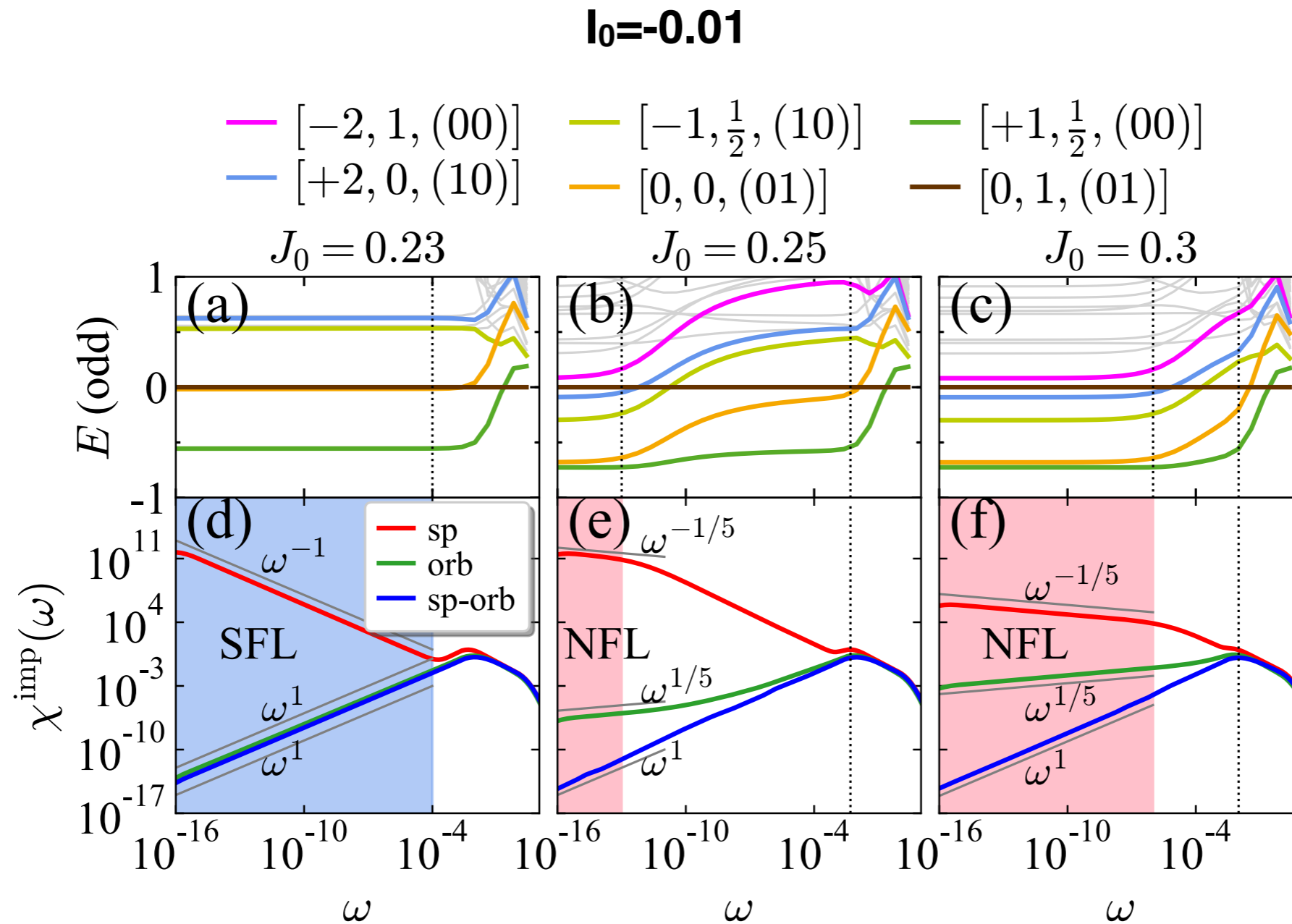
Multiplets	$E_{NFL'}$	E_{FL}	E_{NFL}
$q \ S \ (\lambda_1 \lambda_2) \ d$	@ $I_0 = -0.00609896199692$	@ $I_0 = -0.006098$	@ $I_0 = -0.006099$
$+1 \ \frac{1}{2} \ (00) \ 2$	-0.717930		-0.729529 ($= E_g$)
$0 \ 0 \ (01) \ 3$	-0.668562		-0.680530
$-2 \ 0 \ (00) \ 1$	-0.550738	-0.551028 ($= E_g$)	
$-1 \ \frac{1}{2} \ (10) \ 6$	-0.282883	-0.275517 ($\simeq E_g + \epsilon_e$)	
$-1 \ \frac{1}{2} \ (10) \ 6$	-0.275324		-0.295054
$+2 \ 0 \ (10) \ 3$	-0.0880684		-0.100011
$0 \ 1 \ (01) \ 9$	0	0 ($\simeq E_g + 2\epsilon_e$)	
$0 \ 0 \ (20) \ 6$	0.000037	0 ($\simeq E_g + 2\epsilon_e$)	
$0 \ 1 \ (01) \ 9$	0.011703		0
$-2 \ 1 \ (00) \ 3$	0.102149		0.089692
$+1 \ \frac{3}{2} \ (00) \ 4$	0.275407	0.275518 ($\simeq E_g + 3\epsilon_e$)	
$+1 \ \frac{1}{2} \ (11) \ 16$	0.275410	0.275518 ($\simeq E_g + 3\epsilon_e$)	
$+1 \ \frac{1}{2} \ (11) \ 16$	0.313029		0.300831
$-1 \ \frac{1}{2} \ (02) \ 12$	0.416507		0.404921
$-2 \ 0 \ (11) \ 8$	0.451411		0.439442
$+2 \ 1 \ (10) \ 9$	0.550783	0.551033 ($\simeq E_g + 4\epsilon_e$)	
$+2 \ 0 \ (02) \ 6$	0.550791	0.551033 ($\simeq E_g + 4\epsilon_e$)	

FL and NFL subspaces are orthogonal, both contribute to dynamical and thermodynamical properties, the effective impurity degrees of freedom in NFL' is the *sum* of those two sectors

$$S_{\text{imp}}^{NFL'} = \ln(e^{S_{\text{imp}}^{SFL}} + e^{S_{\text{imp}}^{NFL}}) = \ln\left(1 + \frac{1 + \sqrt{5}}{2}\right)$$

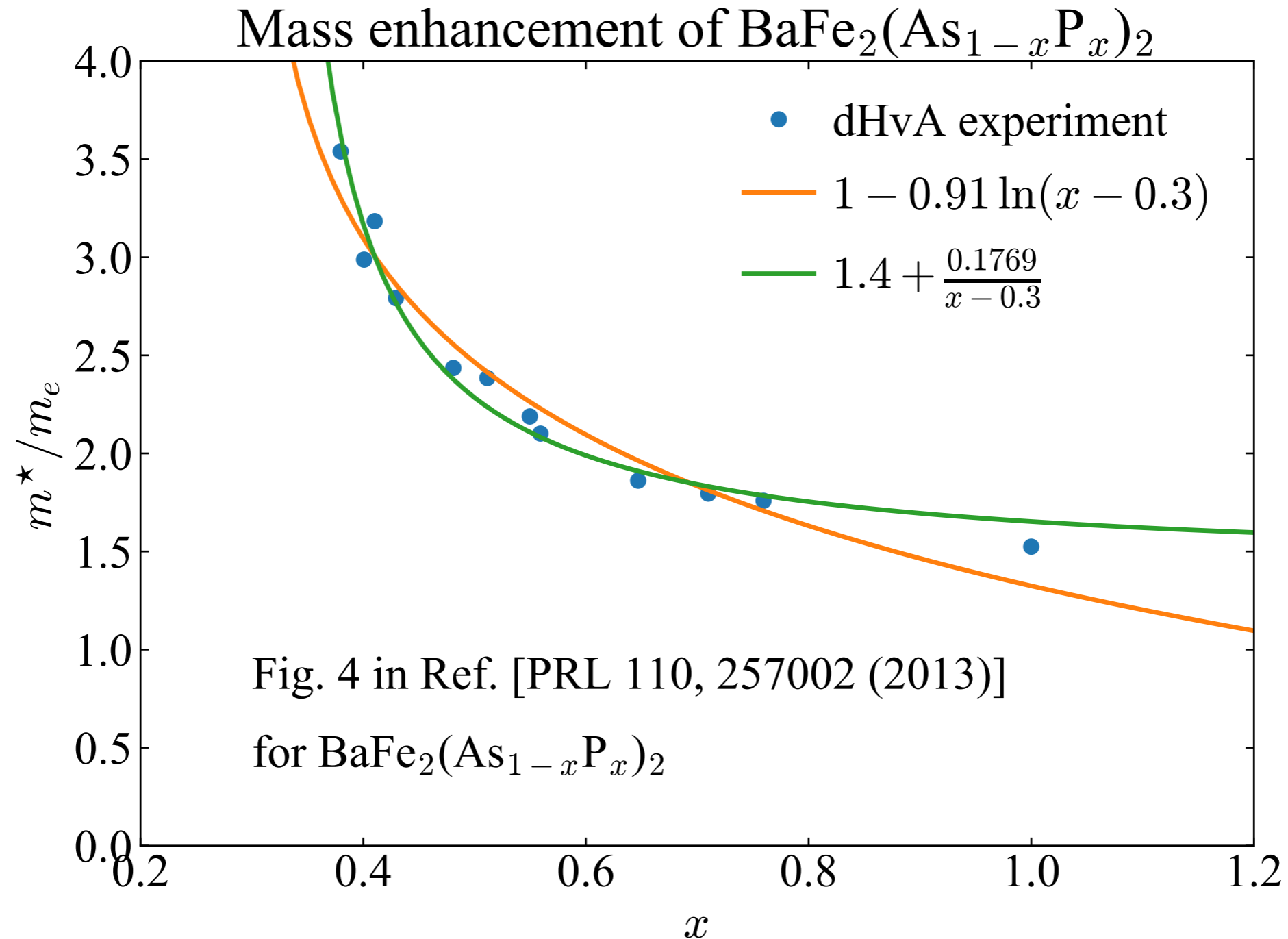
$$\text{not } \ln 1 + \ln \frac{1 + \sqrt{5}}{2}$$

SFL to NFL transition



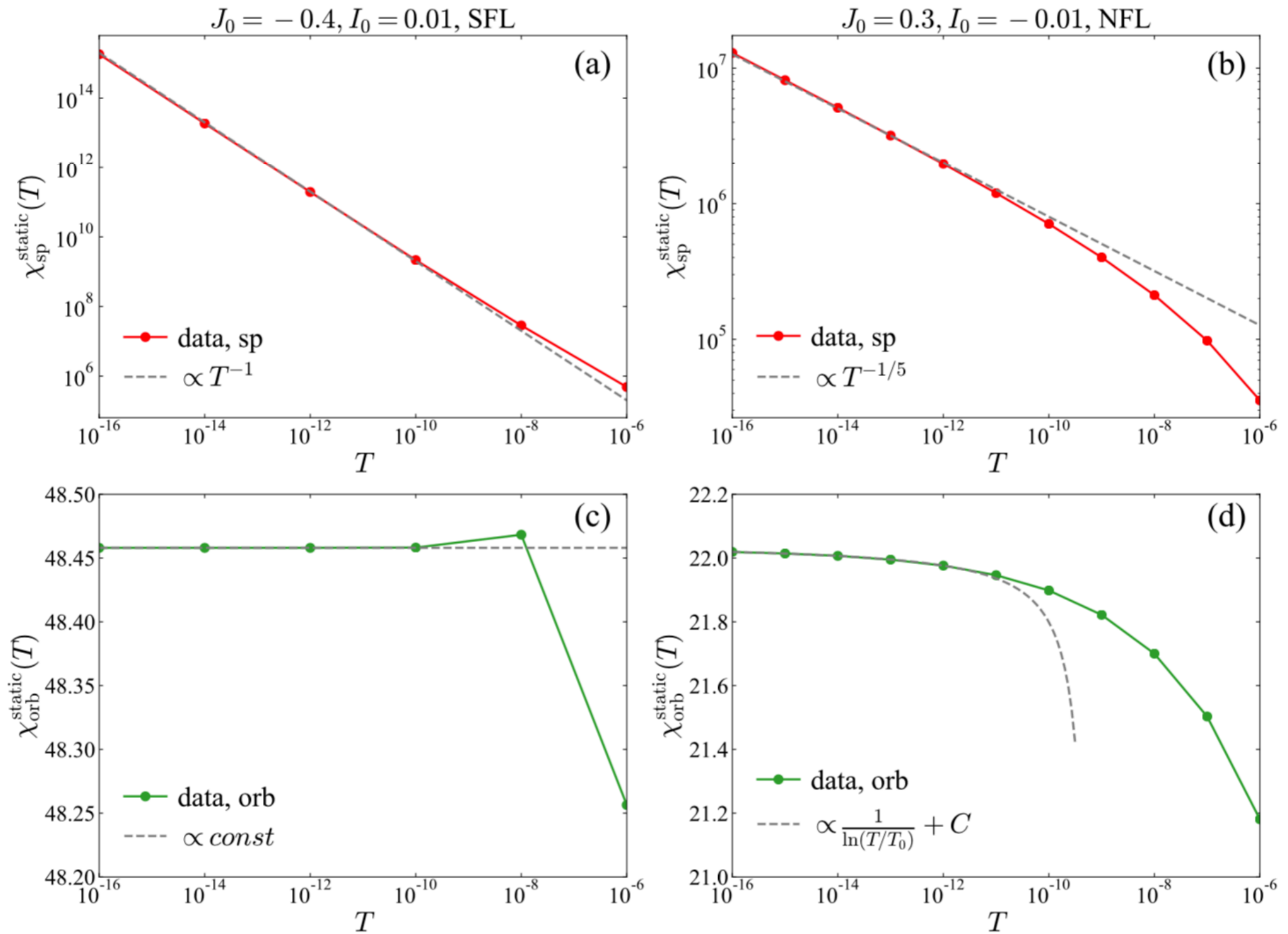
$$[+1, \frac{1}{2}, (00)] \otimes [-1, \frac{1}{2}, (01)] \rightarrow [0, 0, (01)]$$

Connection to the QCP in $\text{BaFe}_2(\text{As}_{1-x}\text{P}_x)_2$



mass enhancement $\propto 1/T_{\text{FL}} \propto 1/(x-x_c)$,
suggests approaching to the NFL QCP

Connection to experiments: Static impurity susceptibilities as functions of temperature T



Summary

- We calculated a global phase diagram of the 3soK model relevant for Hund metal by NRG method, **two new QCPs are identified** by tuning spin and spin-orbital couplings into the ferromagnetic regimes
- **T_{FL} follows power-laws to approach zero energy close the QCPs, this allows us to follow the suppression of the coherence scale in Hund metals down to zero energy**
- We find quantum phase transitions to a SFL and a novel NFL phase. **The NFL phase shows interesting alternating overscreenings in spin and orbital sectors with universal power-laws in dynamical susceptibilities**, and we understand it by powerful CFT arguments. The NFL phase contains the essential ingredients to understand the incoherent behavior seen above **T_{FL}**
- The NFL QCP presented in this work can be used to understand the mass divergence observed in iron pnictides doped with phosphorus
- The approach presented in this work can be generalized to study the unconventional quantum phase transitions observed in other heavy-fermion systems

Thank You !